공학석사 학위논문

Electrochemical Carbon Dioxide Reduction to Methyl Formate in Methanol

메탄올 전해질에서 전기 화학적 이산화탄소 환원으로 메틸포르메이트 생산에 관한 연구

2020년2월

서울대학교대학원

재료공학부

Yeo Jia Bin

(여지아빈)

Electrochemical Carbon Dioxide Reduction to Methyl Formate in Methanol

지도 교수 남기태

이 논문을 공학석사 학위논문으로 제출함

2020년 2월

서울대학교 대학원

재료공학부

Yeo Jia Bin

Yeo Jia Bin의 석사 학위논문을 인준함

2020년 2월

위원장	장지영	
부위원장	남기태	
위원	안철희	

Abstract

Electrochemical Carbon Dioxide Reduction to Methyl Formate in Methanol

Yeo Jia Bin

Department of Materials Science and Engineering

The Graduate School

Seoul National University

Atmospheric carbon dioxide levels have been steadily on the rise since the Industrial Revolution, bringing along the phenomenon of global warming, leading to extreme climate changes, melting of ice caps, destruction of ecosystems, and many other severe environmental issues. In nature, carbon is released from respiration of living things and is recycled by green plants through photosynthesis. In the dark reactions of photosynthesis, CO_2 is incorporated into the structures of sugars by the Calvin cycle. Taking inspiration from this biochemical reaction, an artificial electrochemical CO_2 reduction system utilizing renewable energy sources is proposed to reduce atmospheric carbon dioxide levels and to convert CO_2 to various useful forms. Electrochemical CO_2 reduction research has been mostly done in aqueous electrolyte, and the major reaction products are identified as carbon monoxide,

formic acid, methanol, methane and some highly reduced products such as ethylene and ethanol. The large number of electrons required in CO_2 reduction to ethylene results in low price per electron, and sufficiently high Faradaic efficiencies for economically viable ethylene production from CO2 reduction is yet to be achieved. While carbon monoxide and formic acid have the highest prices per electron, carbon monoxide is highly toxic and requires special handling, and the separation of formic acid from aqueous electrolytes is very difficult due to the formation of an azeotrope. Thus, we turned to a new strategy of CO_2 reductive functionalization to produce new reaction products from CO_2 reduction by the formation of C-C, C-N and C-O bonds. In the case of C-O bond formation, CO_2 is reacted with methanol over a transition metal catalyst at high pressure conditions to form methyl formate. Instead of thermal methods, electrochemical methods have advantages over thermal methods in terms of reaction product tunability, recyclability of the heterogeneous catalyst and mild reaction conditions. Thus, we propose the electrochemical reduction of CO_2 in methanol for the production of methyl formate as a value added product that is easily separable from the reaction solvent.

In order to conduct the experiments in a one-pot cell, an anodic material that does not produce methyl formate from methanol oxidation was selected. Methanol partial oxidation to methyl formate is known to occur on platinum surface, thus the commonly used Pt anode in electrochemical CO_2 reduction systems could not be used in the system to investigate CO_2 reduction in methanol to methyl formate in a one-pot cell. Titanium was found to show little to none methyl formate formation and was thus selected as the anode material in further experiments. For the cathode material, metals not active in CO_2 reduction, CO producing metals, formate producing metals and also hydrocarbon producing Cu were tested and it was determined that Sn showed the highest methyl formate efficiency, thus Sn was chosen as the

cathode material for further experiments. The formation of methyl formate from CO_2 reduction was directly confirmed by isotopic $^{13}CO_2$ experiments. The activity of CO_2 reduction on Sn surface in methanol with sodium perchlorate ($NaClO_4$) supporting electrolyte was confirmed by cyclic voltammetry, and the Faradaic efficiency of methyl formate was fairly unaffected by applied potential and was determined to be 11% to 13% in the range of -1.9V to -2.5V vs Ag/Ag^+. The presence of moisture was also shown to be detrimental to the formation of methyl formate from CO_2 reduction in methanol. In attempt to increase methyl formate Faradaic efficiency, other supporting electrolytes were tested. The effect of the type of cation was tested and it was determined that Na^+ cations yields the highest current efficiency for methyl formate in comparison to Li^+ and TBA^+. The effect of anions was also investigated. BF_4^- anions were determined to yield even higher Faradaic efficiencies in comparison to ClO_4^- anion. It is hypothesized that weakly coordinating anions that have little to none interaction on the cathodic surface are crucial to the formation of methyl formate on Sn surface. Further potential dependency experiments in 0.1M $NaBF_4$ methanol showed methyl formate formation at high current efficiencies at 69% to 79% in the potential range of -2.2V to -2.7V vs Ag/Ag^+.

Key words: Electrochemical CO_2 Reduction, Methanol, Methyl Formate, Reductive Functionalization

Student Number: 2018-18752

Contents

List of Tables

List of Figures

Chapter 1. Introduction

1.1 The Global Carbon Cycle

Carbon dioxide (CO_2) is a well-known greenhouse gas that traps heat in the Earth's atmosphere, keeping the Earth warm. Atmospheric CO_2 levels have been steadily on the rise since the Industrial Revolution in the 19th century. There has been a sharp increase especially in recent years due to excessive carbon dioxide release from industrial activities such as product manufacturing. According to data published by NASA, obtained from the Mauna Loa Observatory, atmospheric CO_2 levels have surpassed a 400ppm threshold in the year 2014, as shown in **Figure 1.1**. This rapid increase in atmospheric CO_2 levels has a close correlation with increase in global temperatures, leading to environmental problems of global warming and climate change.

In attempt to tackle the problem of climate change, global agreements have been signed. The Paris Agreement, for example, has been initially signed in December 2015 and has been adopted under the United Nations Framework Convention on Climate Change (UNFCCC). The aim of the agreement is to keep global warming to well below 2 degrees Celcius and to make efforts to limit increases in global temperatures to below 1.5 degrees Celcius. Countries involved have agreed to submit Intended Nationally Determined Contributions (INDC) to outline their strategies to address a wide range of climate change issues, for example their targets and actions for reducing greenhouse gas emissions. [1] In spite of the many efforts taken by the international community, more in depth research is still needed to tackle global warming from the more fundamental scientific levels.

Shown in **Figure 1.2** is a simplified scheme of the atmospheric carbon cycle. The numbers indicate the amount of carbon released into or absorbed from the atmosphere per year in units of teragrams (Tg/year). Carbon release into the atmosphere through natural processes such as the respiration of living things and the decomposition of organic materials are balanced by natural carbon uptaking processes such as the photosynthesis of green plants. However, human activities such as industrial manufacturing activities have largely lead to increase in CO_2 release into the atmosphere. The burning of fossil fuels to provide energy required for such activities have led to an approximate of 1774 Tg of carbon released per year into the atmosphere, in addition to other carbon emission sources, resulting in a net increase in atmospheric CO2 content by about 1009 Tg of carbon per year.

This leads to an unclosed carbon cycle due to the insufficient uptake of atmospheric carbon by natural processes, leading to an unprecedented increase in atmospheric gaseous carbon levels, consequentially worsening the global warming and climate change scenario. In nature, photosynthesis is the process which enables the capture of atmospheric CO_2 and converting CO_2 into hydrocarbons. Figures 1.3 (a) and (b) show the process of the absorption of CO_2 into the chloroplasts of green plants, which then undergoes the Calvin cycle to incorporate the CO_2 molecule into the structure of sugars, such as glucose. The process of photosynthesis can be expressed in the net reaction:

$$6CO2 + 6H2O + light \rightarrow C6H12O6 + 6O2$$

Taking inspiration from the natural process of photosynthesis, artificial methods to mimic the bioprocesses can be developed to further reduced atmospheric carbon content at a faster rate so as to close the carbon cycle.

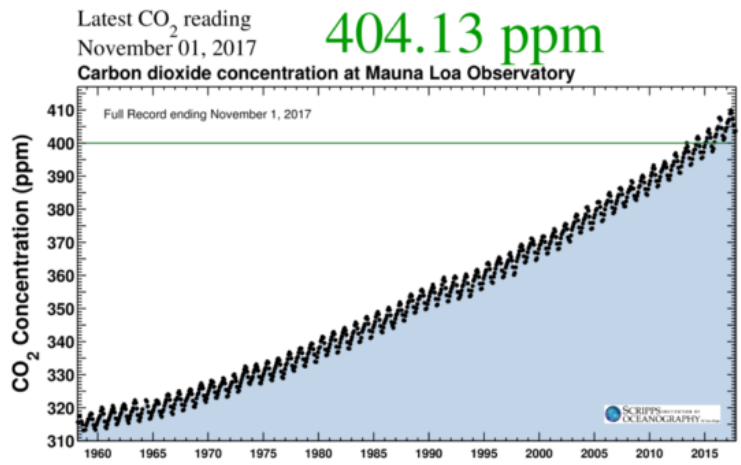

Figure 1.1: Atmospheric CO2 concentrations since the 1960's to 2017. Measurements taken at the Mauna Loa Observatory in Hawaii.

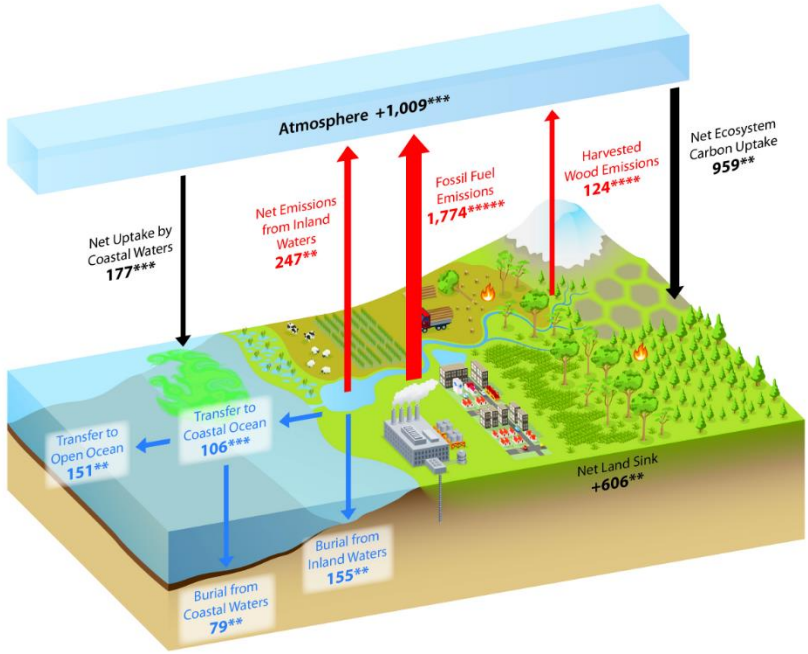

Figure 1.2: The carbon cycle, showing net carbon emission sources and uptake in the environment. The amount of carbon emission and uptake are shown in units of teragrams per year (Tg/year), resulting with a final net increase in atmospheric carbon dioxide amount by 1009 Tg/year.

(a)

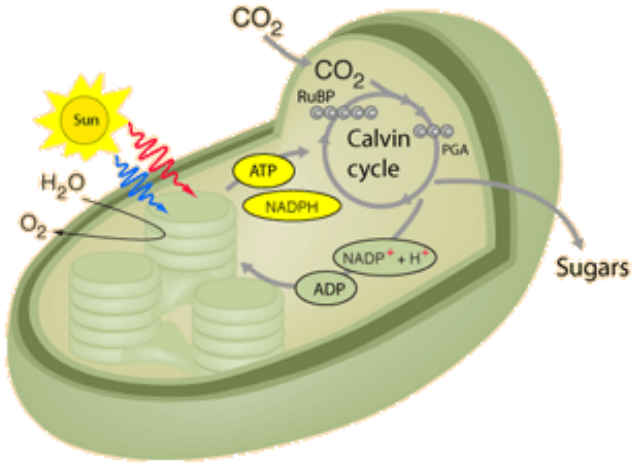

(b)

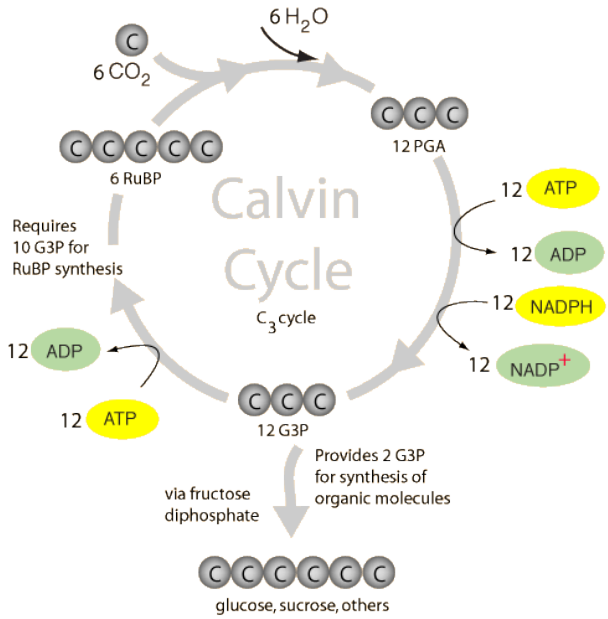

Figure 1.3 (a) A simplified scheme showing uptake of CO_2 in the chloroplast of green plants to be converted to sugars by the Calvin cycle, with the utilization of enzymes and sunlight. (b) The Calvin cycle.

1.2 Electrochemical CO_2 Reduction

Taking inspiration from the natural process of photosynthesis to capture and utilize atmospheric CO_2, artificial methods to capture and utilize atmospheric CO_2 can be developed to balance out the excessive gaseous carbon released from fossil fuel burning. One method is by electrochemical CO2 reduction to other useful chemical forms. Shown in **Figure 1.4** is a simplified scheme for electrochemical CO_2 reduction, in which if renewable, carbon free energy sources can be coupled with the electroreduction system, CO_2 can be chemically reduced to industrially useful chemicals, such as carbon monoxide, formic acid and ethylene, or to fuels, such as methane and methanol, thereby closing the carbon loop. [2,3,4] While CO2 reduction can be achieved by chemical or thermal methods with homogeneous catalysts, electrochemical reduction provides the advantages of using heterogeneous catalysts with high recyclability and separation from the electrolyte, tunability of reaction products, and allows engineering of the catalyst to allow high product selectivity. [5,6]

The CO_2 molecule however, is in the fully oxidized form, which makes it very stable and requires high overpotentials to chemically reduce it to more reduced forms. Listed below are the chemical equations and standard electrode potentials for the reduction of CO_2 to other carbon-based products, estimated from thermodynamic data in aqueous media at 25℃ with respect to Standard Hydrogen Evolution (S.H.E) reference electrode: [7,8,9]

$CO_2 + 2H^+ + 2e^- \rightarrow CO + H_2O$ E°’ = -0.53V

$CO_2 + 2H^+ + 2e^- \rightarrow HCOOH$ E°’ = -0.61V

$CO_2 + 6H^+ + 6e^- \rightarrow CH_3OH + H2O$ E°’ = -0.38V

$CO_2 + 8H^+ + 8e^- \rightarrow CH_4 + 2H_2O$ E°’ = -0.24V

$2CO_2 + 12H^+ + 12e^- \rightarrow C_2H_4 + 4H_2O$ E°’ = -0.34V

Electrochemical CO_2 reduction on various metal electrodes have been widely studied in various systems, which can largely be divided into the aqueous solvent system and the non-aqueous solvent system.

1.2.1 The Aqueous System

Electrochemical CO_2 reduction on various transition metal catalysts are mostly studied and the product distributions are largely established based on the aqueous system. Transition metal catalysts such as copper, zinc, gold, iron and so on are used as the cathode material to test for their CO_2 reduction activity in aqueous medium, mostly with $KHCO_3$ as the supporting electrolyte. Hori's research group have categorized the studied transition metal catalysts into four main categories: [10]

Group 1: CO producing metals – Au, Ag, Zn, Pd, Ga

Group 2: Formate producing metals – Pb, Hg, In, Sn, Cd, Tl

Group 3: Hydrocarbon producing metal – Cu

Group 4: Metals inactive for CO_2 reduction – Ni, Fe, Pt, Ti

Based on this categorization, depending on the target product, specific metals are selected as the electrocatalyst to be studied and many catalyst engineering efforts have been reported to increase the product selectivity and to lower the overpotential for CO_2 reduction to the desired products. [11, 12, 13, 14, 15] Jia et. al., for instance, reported a Cu-Au catalyst for the production of alcohols (methanol and ethanol) from CO_2 reduction in aqueous electrolyte. [16] Le at. al. on the other hand, reported the formation of methanol from CO_2 reduction on copper oxide surfaces at Faradaic efficiencies as high as 38%. [17] While the achieved efficiencies are yet to be high enough for commercialization, these research efforts provide many insights into catalyst

design and engineering that can be attempt to achieve selective CO_2 reduction to value added products at high efficiencies.

Hydrocarbon products such as ethylene are considered to be highly valuable and much research focus into the selective production of ethylene from CO_2 reduction using copper based catalysts have been attempted. [18, 19, 20, 21] The highest reported current efficiency for ethylene has been done by H. Mistry about an oxygen plasma treated Cu catalyst for the selective production of ethylene from CO_2 reduction. The oxygen plasma treatment can be adjusted to manipulate the catalyst surface for more selective ethylene formation. The overpotential for ethylene formation in aqueous solution was reported to be lowered to -0.9V vs R.H.E and the highest ethylene Faradaic efficiency or product selectivity was improved to 60% (**Figure 1.5**). [18]

Carbon monoxide (CO) is another valuable product from CO_2 reduction that is industrially important for the manufacture of various chemicals. Highly selective catalysts have been developed based on CO producing metals such as Ag, Au, and even bimetallic catalysts such as Pd-Cu. [22, 23, 24, 25, 26] One of the most facile fabrication method with very high CO current efficiency instance was reported by Q.Z. Li about an anodized polycrystalline Ag electrode to reduce CO_2 to CO at a low overpotential of 0.5V at a high selectivity of 92.8% (**Figure 1.6**). The selectivity was reported to be due to a preferred (220) orientation and the thin oxide layer due to anodization on the catalyst surface. [22]

Formate or formic acid is important as fuel for direct formic acid fuel cells, or as reactant for other chemical synthesis. Selective formate producing catalysts also have been developed based on formate producing transition metals such as Sn, Pb and Bi. [27, 28, 29, 30, 31,32, 33, 34] Lee et. al. reported a Bi-based catalyst for selective formate production from CO_2 reduction in aqueous electrolyte. The carbon-supported BiO_x nanoparticles showed formate current efficiencies as high as 93.4% in bicarbonate solutions, while

current efficiencies as high as 96% was achieved in NaCl solutions as shown in **Figure 1.7**. [34]

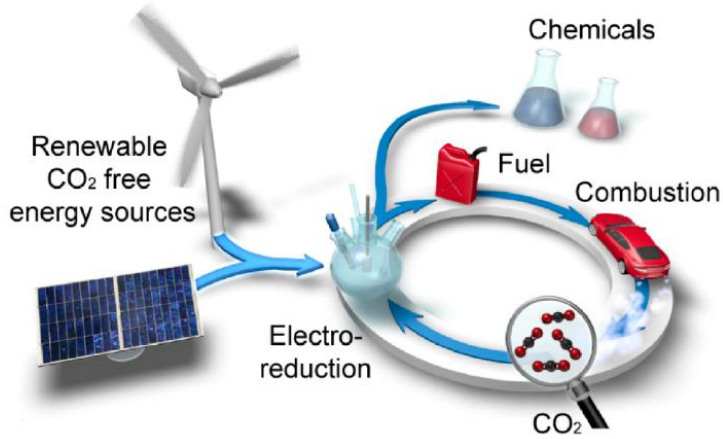

Figure 1.4: Scheme showing electrochemical CO_2 reduction to fuels and industrially useful chemicals, coupled with renewable CO_2 free energy sources to create a CO_2 neutral energy cycle.

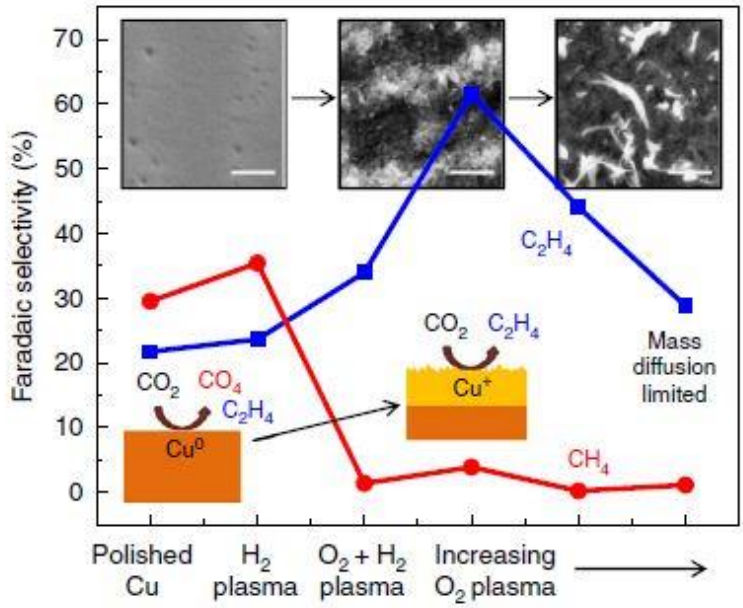

Figure 1.5: Oxygen plasma treated copper catalyst for selective C_2H_4 formation.

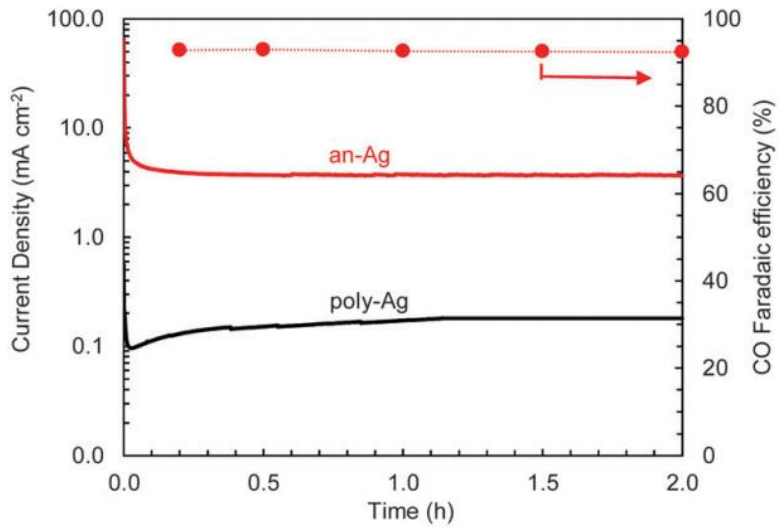

Figure 1.6: Anodized Ag electrode for highly selective CO formation.

(a)

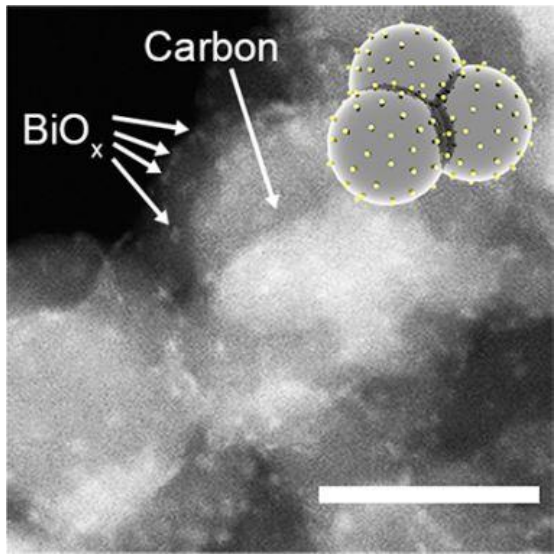

(b)

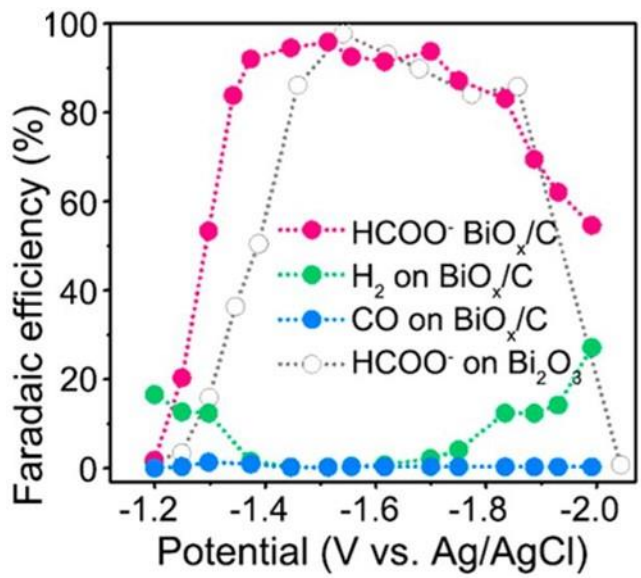

Figure 1.7: (a) STEM image of carbon supported BiOx nanoparticles and (b) Potential dependence of Faradaic Efficiencies for HCOO-, H2, and CO production on the BiO_x/C catalysts and commercial Bi_2O_3.

1.2.2 The Non-Aqueous System

Electrochemical CO_2 reduction in the non-aqueous system has also been researched as an alternative system to the aqueous system. Since CO_2 solubility in non-aqueous organic solvents are much higher than in water at ambient pressure and temperature conditions, CO_2 reduction is expected to occur at higher selectivity and hydrogen evolution reaction (HER) is expected to be suppressed compared to the aqueous system. Table 1 shows the solubility of CO2 in various solvents at 25℃. [35] Methanol has 5 times higher CO_2 solubility compared to water, while organic solvents such as acetonitrile (ACN) and dimethylformamide (DMF) has 6 to 8 times higher CO_2 solubility.

The electrochemical reduction of CO_2 in non-aqueous organic solvents however did not yield hydrocarbon products as in the aqueous solvent system due to the lack of proton donors in organic solvents. S. Ikeda reported selective formation of oxalic acid and carbon monoxide in organic solvents, which are propylene carbonate (PC), DMSO and ACN. The formation of oxalic acid is reported to be highest when Pb is used as the electrocatalyst in all 3 organic solvents (73% in PC and 65% in DMSO and ACN), while CO is produced the most selectively on In also in all tested organic solvents (85% in PC, 90% in DMSO, and close to 100% in ACN). [36]

Despite these reports, electrochemical CO_2 reduction in organic solvents is currently less explored compared to aqueous solvents. Since the reacting system is fundamentally different compared to aqueous system, other new reaction products can still be possibly formed and thus opens up further exciting new possibilities for electrochemical CO_2 reduction. [37, 38, 39, 40]

Solvent	Concentration (M)/conditions
Water	0.33
Methanol	0.06
Tetrahydrofuran (THF)	0.205 ± 0.008
Acetonitrile (ACN)	0.279 ± 0.008
Dimethylformamide (DMF)	0.199 ± 0.006
Dimethylsulfoxide (DMSO)	0.138 ± 0.003

Table 1.1: Solubility of CO2 in various solvents at 25℃.

1.2.3 Challenges in Electrochemical CO_2 Reduction

While the major products of electrochemical CO_2 reduction in aqueous solvents have been well identified, which are carbon monoxide, formic acid or formate, methanol, and also some highly reduced products such as ethylene and ethanol, the value of the products vary greatly. Highly reduced products, especially ethylene, is often regarded as highly value added and much focus on research has been given to improving Faradaic efficiency to produce ethylene from CO_2 reduction.

Considering the price of the major CO_2 reduction products, ethylene indeed has the highest market price among other less reduced products such as carbon monoxide and formic acid, as shown in Table 1.2. [41] However, considering the normalized price, or the price per electron involved in the reaction, the price of ethylene ($1.3 x 10^3/electron) is actually much lower than that of carbon monoxide ($8.0 x 10^3/electron) and formic acid ($16.1 x 10^3/electron).

Furthermore, while highly selective CO and formic acid producing catalysts have been widely researched and developed, and very high Faradaic efficiencies of these products have been achieved, the Faradaic efficiencies achieved for highly reduced products like ethylene and ethanol remains low to this day, as shown in Figure 1.8. [41] While many attempts to develop catalysts to selectively produce ethylene and ethanol, high Faradaic efficiencies for these value added products remain elusive and thus, difficult to be commercialized. [42, 43, 44]

In order to evaluate the economic viability of these CO_2 reduction products, the Net Present Value (NPV) of the chemicals at a defined overpotential and the achieved Faradaic efficiency is considered. For a reaction product to be economically feasible, the NPV of the product needs to be greater than zero.

Products like carbon monoxide and formic acid has been shown to be economically viable at all overpotentials, while for ethylene and ethanol, considering a reasonable overpotential at 0.7V, the Faradaic efficiency has to be at least 89% and 77% respectively for the NPV to be greater than zero, as seen in Figure 1.9 [12]. Such high Faradaic efficiencies for ethylene and ethanol has yet to be achieved, and thus these products are deemed to be economically not viable for the moment.

While the major reaction products for CO_2 reduction have been mostly identified, there are still challenges in realizing electrochemical CO_2 reduction in an economically viable sense. While highly reduced products such as ethylene is valuable, economic viability remains low. Even though CO and formic acid are economically viable products, CO is highly toxic and requires special care in handling, and formic acid, or formate are difficult to separate from aqueous electrolytes. [45, 46, 47, 48] Thus, a different strategy is required to obtain new value-added products from CO_2 reduction. New products or chemicals can possibly be synthesized from CO_2 if a new strategy is adopted by using non-aqueous solvents or by coupling with other chemicals.

(a)

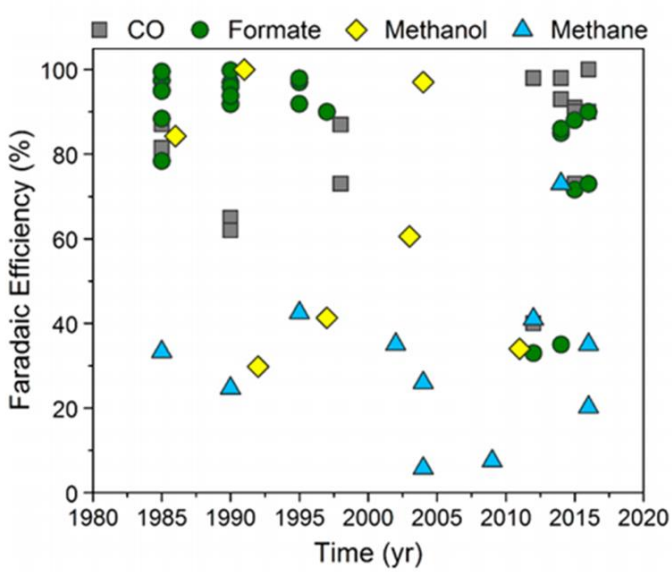

(b)

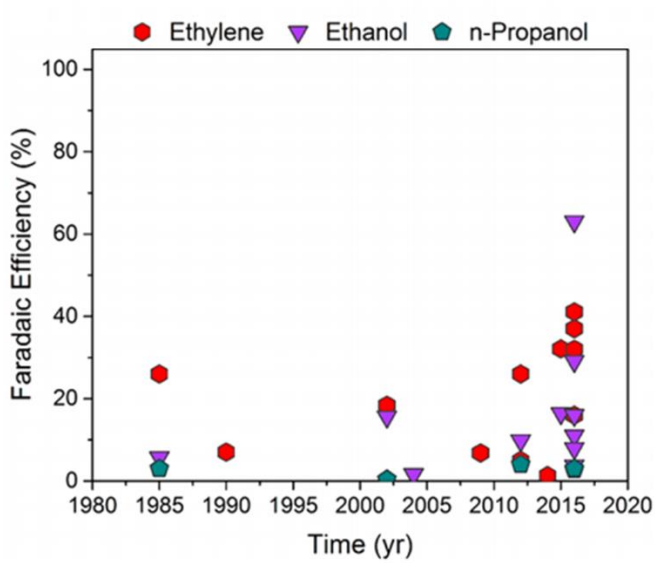

Figure 1.8: Faradaic efficiencies of (a) CO, formate, methanol, methane and (b) ethylene, ethanol, n-propanol achieved from years 1980 to 2019.

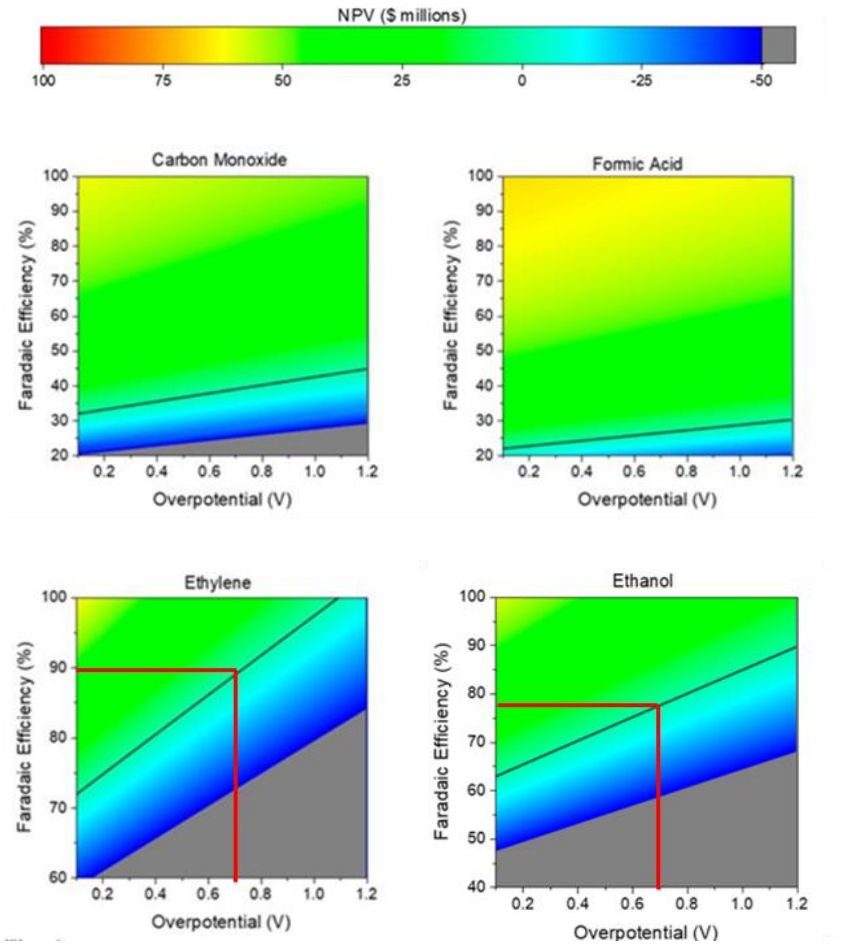

Figure 1.9: Net Present Value (NPV) plots for CO_2 reduction products (carbon monoxide, formic acid, ethylene and ethanol) at various applied overpotentials and the achievable Faradaic efficiencies.

Product	Number of Required Electrons	Market Price ($/kg)	Normalized Price ($/electron) x 10^3
CO (syngas)	2	0.06	0.8
CO	2	0.6	8.0
Formic acid	2	0.74	16.1
Methanol	6	0.58	3.1
Methane	8	0.18	0.4
Ethylene	12	1.30	3.0
Ethanol	12	1.00	3.8
n-Propanol	18	1.43	4.8

Table 1.2: Market price and normalized price of CO_2 reduction products.

1.3 CO_2 Reductive Functionalization

CO_2 reductive functionalization is a new perspective that has been gaining much interest of late. Instead of direct reduction of CO_2, CO_2 recycling can be achieved in the vertical way or the horizontal way as shown in Figure 1.10 [49, 50, 51, 52, 53]. The vertical approach is the direct reduction of CO_2 to more reduced forms like methanol and methane. The more reduced the product, the higher the energy density of the product, and the oxidation number of the carbon center increases. In contrast, the horizontal approach can be done by pairing with amine groups or carbonate groups to form urea or dicarbonates. However, the oxidation number of the carbon center remains unchanged in the horizontal utilization, thus the energy density of the chemicals formed in this manner has low energy density and are typically not used as fuels as the more reduced chemical forms are.

In between the vertical and horizontal approaches, there is the diagonal utilization or reductive functionalization of CO_2. Reductive functionalization of CO_2 is achieved by pairing of a reduced form of CO_2 with other functional groups to produce a wide range of organic molecules such as esters and amines by the formation of C-C, C-N and C-O bonds. Such reports of C-C, C-N and C-O bond formations so far are all achieved by thermal methods.

An example of C-C bond formation is the production of benzaldehyde from CO2 and halobenzene by a Pd molecular catalyst at ambient pressure as shown in Figure 1.11 (a). A C-N bond example is shown by the formation of dimethylformamide or diethylformamide from the coupling between CO_2 and dimethyl amine and diethyl amine respectively as shown in Figure 1.11 (b). Also, C-O bond formation is exemplified by the coupling between CO_2 and methanol to form methyl formate.

1.3.1 C-O Bond Formation by Production of Methyl Formate

As shown in the previous section, formic acid is a valuable product and has high normalized price per electron. The production of formic acid or formate from CO_2 reduction in aqueous electrolyte however presents an unexpected problem. Formic acid is difficult to separate from the aqueous electrolyte due to the formation of an azeotrope, which is a liquid mixture that maintains its composition and boiling point during distillation, as formic acid and water have very similar boiling points (100.8℃ and 100℃ respectively). Formic acid and water mixture separation becomes complicated when special techniques such as extractive distillation, in which the extractive distillation agent used is a sulfone, is required. This adds on to the costs of production of formic acid from CO_2 reduction in aqueous electrolyte, even if high Faradaic efficiencies can be achieved with the reported catalysts.

Formic acid however, is known to react easily with methanol by esterification reaction to form methyl formate. The esterification reaction between methanol and formic acid occurs readily at slightly elevated temperatures (ca. 60℃) in the presence of an acid catalyst such as sulphuric acid. If CO_2 reduction is conducted in methanol electrolyte, the resulting methyl formate and methanol mixture can be easily separated by slight heating due to the large differences in their boiling points (31.5℃ and 64.7℃ respectively).

Furthermore, methyl formate has the highest market price ($20/kg) in comparison with methanol ($0.58/kg) and formic acid ($0.74/kg). By the production of methyl formate from CO_2 reduction, value addition can be achieved from reacting materials with low cost such as methanol. The normalized price per electron of methyl formate as a reaction product is also not decreased since the formation of formic acid or formate as an intermediate species requires only 2 electrons per molecule formed, in comparison with 12 electrons that is required for the formation of ethylene.

Methyl formate has a wide range of industrial applications and has a wide range of chemistry, thus is considered as a building block molecule in C1 chemistry. Methyl formate is used as a precursor chemical for several industrially important chemicals. By reacting with ammonia (NH_3) at 80 to 100℃ and elevated pressures at 400 to 600kPa, formamide ($CHONH_2$) can be produced, which is a chemical feedstock for the manufacture of drugs, pharmaceuticals, herbicides, pesticides and also for the manufacture of hydrocyanic acid. Dimethylformamide (DMF, $CHON(CH_3)_2$), which is a commonly used organic solvent, is produced by reacting methyl formate with dimethyl amine ($(CH_3)_2NH$) at 50℃ and 500kPa. Formic acid (HCOOH), which is used as fuel in direct methanol fuel cells, and also as a useful organic synthetic reagent, can be manufactured from methyl formate by heating at 25 to 120° over an inorganic acid catalyst. The rich chemistry of methyl formate also allows it to be used as a building block molecule for various organic molecules. By coupling methyl formate with carbonyl compounds, such as formaldehyde, methyl glycolate ($HOCH_2CO_2CH_3$) can be produced, which can be further reacted to produce malonate ester or polyglycolate, which are useful materials in the medical filed. Methyl formate can also be coupled with olefins such as ethylene ($CH_2=CH_2$) to produce methyl propionate. The halogenation of methyl formate with chlorine produces methyl chloroformate, which when reacted with olefins produces methoxy carbonyl compounds. The oxidation of methyl formate in the presences of sodium methoxide meanwhile, produces dimethyl carbonate. [54]

Methyl formate can be synthesized through many reaction routes. The commercialized method developed by BASF involves the carbonylation of methanol, by reacting CO and CH_3OH in the presence of sodium methoxide as the catalyst, at 60 to 120℃ and 20 to 70 bar CO to produce methyl formate. Other alternative methods, as shown in Figure 1.12, such as the dimerization of formaldehyde in the presence of a Cu or Zn catalyst, the oxidative

dehydrogenation of methanol, the dehydrogenation of methanol or direct synthesis from synthesis gas (syngas) have also been suggested, but these methods have problems with low product yield. Another interesting pathway is by the hydrocondensation of CO_2 with methanol to produce methanol. This method however has a problem as it uses H_2 gas as one of the reactants, which is more expensive than CO gas. [54]

The utilization of CO_2 in the production of methyl formate however, is interesting and relatively unexplored. Previous reports of CO_2 utilization in the formation of methyl formate are all conducted by thermal methods, and some suggests that the formation of methyl formate is the result of the conversion of CO_2 to formic acid and subsequently reacts with methanol to produce methyl formate at high pressure conditions under the presence of a transition metal catalyst. As shown in Figure 1.13, CO_2 is reacted with hydrogen gas as the reducing reagent in the presence of a Fe-based molecular catalyst at high pressure conditions in methanol. Formic acid is suggested to be formed from this reduction. The formic acid then reacts with alcohol, or methanol in this case to form methyl formate. [53]

In this research thesis, electrochemical methods is employed to reduce CO_2 to methyl formate in methanol as the electrolyte. Methyl formate can be achieved in a one-step procedure at ambient pressure and temperature conditions. To the best of our knowledge, electrochemical methods targeting the synthesis of methyl formate utilizing CO_2 as the reactant molecule has yet to be reported.

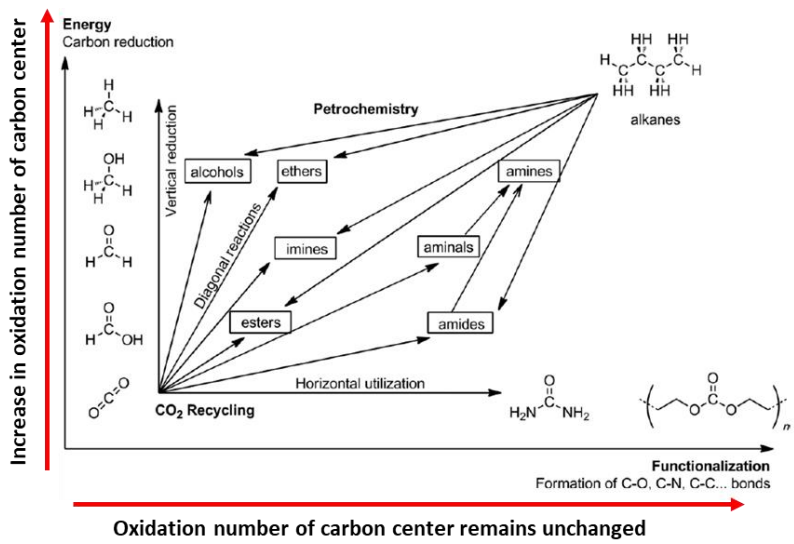

Figure 1.10: Vertical and horizontal utilization, and also reductive functionalization or diagonal utilization of CO_2.

(a)

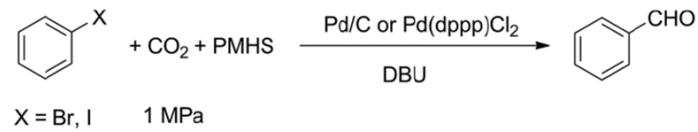

(b)

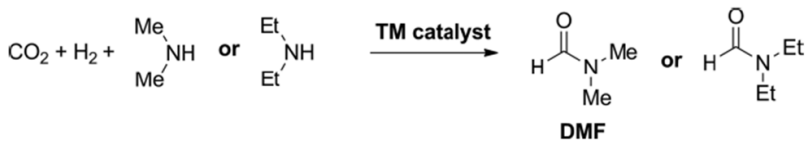

(c)

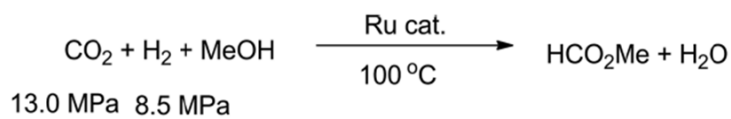

Figure 1.11: (a) C-C bond formation between CO_2 and halobenzene to form benzaldehyde, (b) C-N bond formation between CO_2 and dimethyl amine or diethyl amine to form dimethylformamide or diethylformamide, (c) C-O bond formation between CO_2 and methanol to form methyl formate.

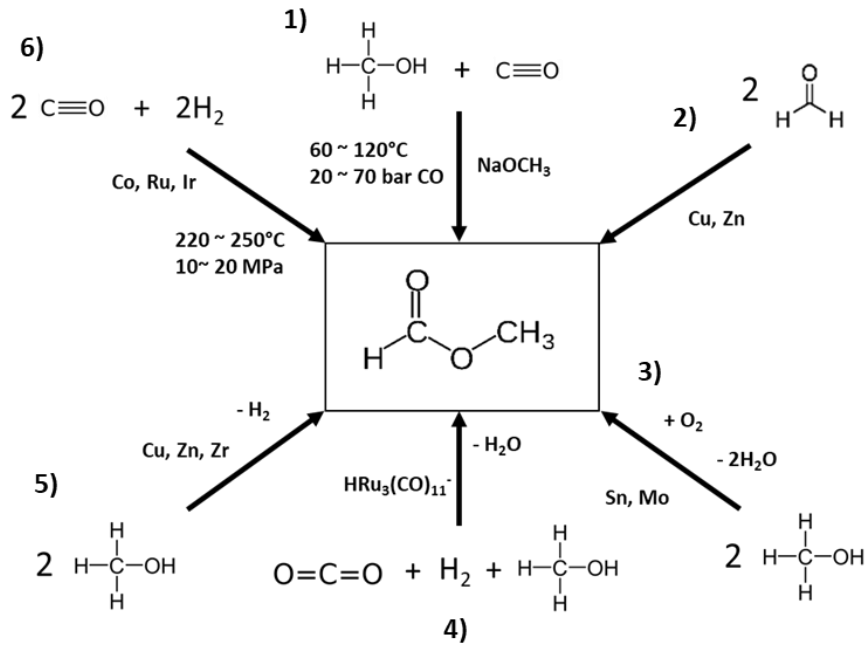

Figure 1.12: Methyl formate synthesis routes – 1) Carbonylation of methanol, 2) Dimerization of formaldehyde, 3) Oxidative dehydrogenation of methanol, 4) Hydrocondensation of CO_2 with methanol, 5) Dehydrogenation of methanol and 6) Direct synthesis from syngas.

Entry	Product	$P(H_2/CO_2)$ [bar]	Yield [%]	TON
1	HCO_2Me	60/30	56	292
2	HCO_2Me	60/30	14	585

Figure 1.13: C-O bond formation between CO_2 and methanol to form methyl formate through a formic acid intermediate.

1.3.2 Methyl Formate Production by Electrochemical CO_2 Reduction in Methanol

A fair amount of research into electrochemical CO_2 reduction in methanol has been conducted since 1993. The starting initiative of conducting electrochemical CO_2 reduction in methanol is due to hopes incorporating the reaction into the Rectisol process, which is a chemical process that is often incorporated into chemical synthesis plants to remove acid gases such as carbon dioxide and hydrogen sulphide from valuable feed gas streams. The Rectisol process is done at low temperature conditions, and since CO_2 solubility in methanol is increased at high pressures as shown in Figure 1.14 [55], majority of the reports of CO_2 reduction are conducted at low temperature or high pressure conditions.

While various transition metal catalysts have been investigated for their reactivity for CO_2 reduction in methanol, there were no particular advantages over CO_2 reduction in aqueous solvent that is being reported. The main products that were produced by CO2 reduction in methanol were mainly the same as in aqueous solvent, which are carbon monoxide, methane, formate or formic acid, and some level ethylene. Furthermore, the Faradaic efficiency achieved in methanol solvent is not much better than in aqueous solvent. [55 – 65]

There were nevertheless, three papers that reported the formation of methyl formate on copper and a number of other transition metals at high pressure conditions.

Saeki et. al. reported the electrochemical reduction of CO2 with high current density in a CO2 methanol medium at various transition metal electrodes at ambient temperature and high pressure conditions (41atm). [59] The reaction products were reported as CO, CH_4, C_2H_4, and methyl formate ($CHOOCH_3$). The resulting product distribution is reported to be similar to as

observed in aqueous systems as shown in Figure 1.15. At W, Ti and Pt electrodes, CO_2 reduction is inactive and hydrogen evolution was prevalent. At Ag, Zn and Pd the main reaction products were CO. Hydrocarbon products (C_2H_4) is produced on Cu surface, but the efficiency is less than that observed in aqueous system. Sn and Pb are known as formate producing metals in aqueous electrolyte. Here, it reported that methyl formate formation is observed instead. The formation of methyl formate is predicted to be formed due to the formation of formic acid on Sn and Pb electrodes, which then reacts with methanol chemically to form methyl formate (Faradaic efficiency of 40% on Sn and 80% on Pb). Note that however in later reports on formate producing metals such as Pb [60] and In [65], in which the reaction was conducted in KOH-methanol medium a ambient pressure and temperature conditions, methyl formate was not reported. Instead, formic acid was reported as the observed product at high current efficiencies (66% on Pb and 76% on In). Despite the high current efficiencies of methyl formate reported at the high pressure conditions, not data confirming the origin of the methyl formate observed is from CO_2 reduction is provided. Of course, the reaction between formic acid formed from CO_2 and methanol to form methyl formate could have easily occurred under high pressure conditions, but the anode material used was Pt, and the reaction cell used was an unseparated one pot cell. It is reported that methyl formate formation from methanol oxidation on Pt surface is observed as shown in Figure 1.16. [66] Thus the reported efficiency of methyl formate could possibly be include the amount of methyl formate that is being produced on the anodic methanol oxidation reaction. Other than methyl formate which is being produced at high efficiencies on Sn and Pb, CO is also observed to be produced at high current efficiencies in comparison with aqueous solvents. Considering the fact that the supporting electrolyte used in these reports were tetrabutylammonium perchlorate (TBAP), it was suggested that the enhanced formation of CO on Sn and Pb was due to the promoting effect of the TBA cation.

Despite that methyl formate formation from CO2 reduction in methanol on Sn and Pb electrodes were reported at high current efficiencies, no further investigations were reported on Sn electrode. Instead, it appeared that ethylene was considered as a more value-added product, and thus CO_2 reduction on Cu surface was given more attention. The only other two papers that reported methyl formate formation at high pressure conditions were obtained on Cu electrode surface. Kimura et. al. reported the electrochemical reduction of CO_2 with high current density in a CO_2-methanol medium with Cu as the electrocatalyst and tetrabutylammonium tetrafluoroborate ($TBABF_4$) as the supporting electrolyte. In this report, the formation of methyl formate was observed to occur at high pressures, and even ambient pressure at current efficiency around 20%. [55]

In another paper by Saeki et. al., electrochemical reduction of CO_2 with high current density in a CO_2 + medium with CO formation promoted by tetrabutylammonium cation was reported. [58] Under 40atm and 25°C, it was observed that electrochemical CO_2 reduction in methanol on Cu surface yielded CO as the main reaction product when $TBABF_4$ and $TBAClO_4$ were used as the supporting electrolyte. Meanwhile, when Li salts such as $LiBF_4$ and $LiClO_4$ were used as the supporting electrolyte, methyl formate was obtained as the major reaction product at Faradaic efficiencies as high as 54.5% and 46.7% respectively. Again, the reported high current efficiencies for methyl formate could be due to the fact that a one-pot cell was employed in the experiments and that a portion of the observed methyl formate current efficiency could originate from the anodic methanol oxidation reaction. The difference between the product distribution when Li salts and TBA salts were used were explained by the hydrophobicity / hydrophilicity of the near cathode surface environment created by the employed cations. It was suggested that the presence of TBA^+ cations resulted in a hydrophobic

environment, in which the CO production was enhanced since CO can be produced without hydrogenation by the reaction:

$CO_2^{-}\cdot + CO_2 + e^- \rightarrow CO + CO_3^{2-}$

Meanwhile when Li salts are used, a hydrophilic environment is formed, leading to the prevalent formation of methyl formate since protonation step is involved in its formation as follows:

$CO_2^{-}\cdot + 2H^+ + CH_3OH + e^- \rightarrow CHOOCH_3 + H_2O$

Li^+ ions are smaller and is considered to be more solvated by methanol than TBA^+, and thus the electrode vicinity may be more hydrophilic than when TBA^+ salts are used. Thus taking hint from the important role of the cation species, metallic cation salts were given priority for investigation.

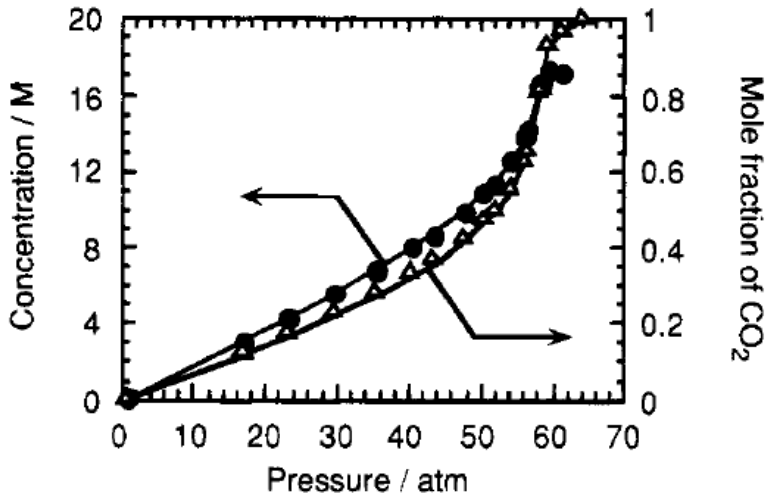

Figure 1.14: Concentration and mole fraction of CO2 in methanol at different applied pressures.

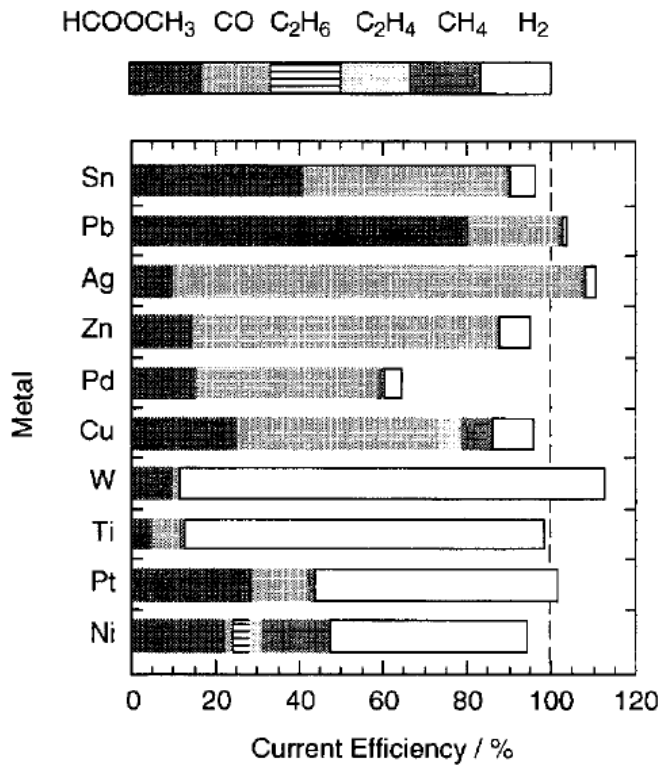

Figure 1.15: The observed product distribution for electrochemical CO2 reduction at 25℃, 41atm on various transition metal electrodes in methanol.

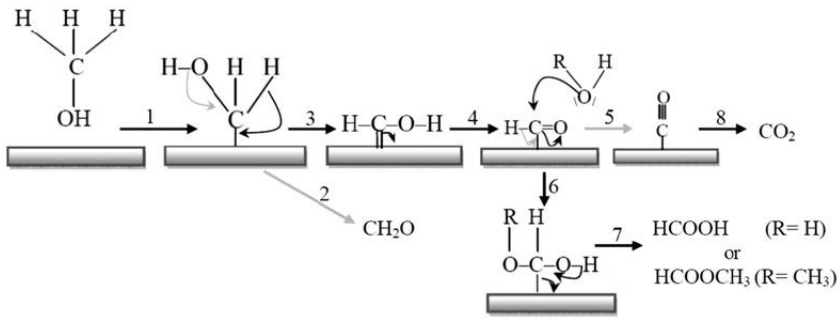

Figure 1.16: The suggested mechanism of the formation of methyl formate from methanol oxidation on Pt surface, which differs from previous reports suggesting that methyl formate formation is due to chemical reaction step between formaldehyde formed from methanol oxidation and a methanol molecule, instead of direct oxidation steps on Pt surface.

Chapter 2: Study on Electrochemical CO2 Reduction to Methyl Formate in Methanol at Ambient Temperature and Pressure

2.1 C-O Bond Formation by the Formation of Methyl Formate by Electrochemical CO2 reduction in Methanol

As previously mentioned in Chapter 1, electrochemical CO_2 reduction on various transition metal catalysts have been investigated. The development and engineering of electrocatalysts, and consequently the study of electrochemical CO_2 reduction on these electrocatalysts have been mostly done in aqueous electrolytes due to the abundance and low cost of using water as the solvent for CO_2. However, the solubility of CO_2 in water is low, and thus non-aqueous electrolytes and ionic liquids have also been considered as electrolytes for CO_2 reduction due to their much high solubility for CO_2. Electrochemical CO_2 reduction in organic solvents however is relatively different from in aqueous solvents due to the lack of a proton source if non is added. Though the major reactant products in aprotic solvents like DMF and propylene carbonate are identified as CO and oxalate, the reaction mechanisms are largely not studied as the use of such organic solvents are also relatively expensive in comparison with water. Electrochemical CO_2 reduction in organic solvents however could offer new possibilities considering the wide range of organic solvents available. New products can possibly be obtained by CO_2 reduction in the organic solvents or by pairing with other chemicals other than the well-established major products obtained from electrochemical CO_2 reduction in aqueous electrolyte, which are CO, formic acid, methane, methanol, and ethylene.

Instead of the direct reduction of CO_2 to more reduced forms, diagonal functionalization or reductive functionalization by coupling a reduced form of CO_2 with other chemicals by the formation of C-C, C-N or C-O bond opens up various new possibilities of new value added products obtainable from CO_2 reduction without the involvement of large number of electrons such as ethylene. The formation of C-O bond is exemplified by methyl formate formation from CO_2 which is predicted to form formic acid, and subsequently reacts with methanol by esterification reaction. CO_2 reductive functionalization however, is reported only by chemical / thermal methods and at high pressure conditions.

Reactions at ambient pressure and temperature conditions are economically more advantageous due to less energy consumption in the reaction process, and thus electrochemical CO_2 reduction at ambient pressure and temperature conditions in methanol to produce methyl formate is attempted. While previous reports on electrochemical CO_2 reduction in methanol has been numerous, only at high pressure conditions that methyl formate formation was reported. Similarly, methyl formate was predicted to be formed through the formate pathway from CO_2 reduction due to the high current efficiencies observed when formate producing metals such as Sn and Pb are used. However, since the reaction cell used in these investigations was a one-pot cell and the anode used was Pt, methanol oxidation on Pt surface could occur and the reported methyl formate Faradaic efficiency may be higher than the actually achieved value.

Thus for the scope this thesis, electrochemical CO_2 reduction in methanol on Sn surface at ambient pressure and temperature conditions was conducted in a one-pot cell with an anode material that has been determined to suppress methyl formate formation. The product distribution, effect of water content, effect of supporting electrolyte, and also a comparison with different transition metal catalysts are discussed.

2.2 Experimental Procedures

2.2.1 Chemicals and Materials

Methyl alcohol (99.9%), sodium perchlorate, sodium nitrate and sodium hydrogen carbonate were purchased from Daejung Chemicals (Gyeonggido, Korea). Lithium perchlorate, sodium hydroxide, sodium sulfate, methyl formate and Nafion N-117 membrane (0.18mm thick) were purchased from Alfa Aesar (MA, USA). Tetrabutylammonium perchlorate, sodium methoxide were purchased from TCI Chemicals (Tokyo, Japan). Sodium chloride was purchased from Sigma-Aldrich (Milwaukee, WI, USA). $^{13}CO_2$ (99%) was purchased from Cambridge Isotope Laboratories Inc. (MA, USA). Methyl alcohol was dried with 3Å molecular sieves (purchased from Daejung Chemicals) for more than 48 hours prior to usage, sodium perchlorate was dried at 220℃ in air for more than 24 hours prior to usage. Other chemicals are opened in Ar environment, stored in glove box and used as received. Tin foil (Sn, 0.25mm thick), titanium foil (Ti, 0.127mm thick), gold foil (Au, 0.1mm thick), lead foil (Pb, 0.25mm thick), indium foil (In, 0.127mm), copper foil (Cu, 0.025mm thick), nickel foil (Ni, 0.1mm thick), platinum foil (Pt 0.025mm thick), glassy carbon plate and mercury acetate ($Hg(O_2CCH_3)_2$) were purchased from Alfa Aesar. Dimensionally Stable Anodes (DSA, Ru oxide coated on Ti) was purchased from Siontech (Daejeon, Korea).

2.2.2 Electrochemical Analysis

An undivided three-electrode cell (Gamry Dr. Bob's cell) was used in all the voltammetric measurements and electrolysis, while a custom-made H-cell with a Nafion 117 membrane (1cm diameter) fitted in between the cathodic and anodic compartment was used in anode material determining experiments. Sn, Ti, Au, Pb, In, and Cu foils with surface dimensions 2cm x

0.5cm x 2 were used as the working electrodes. Hg / Cu amalgam electrode is made by immersing Cu foil with the same dimensions in 0.01M $Hg(O_2CCH_3)_2$ solution for 10 minutes and then taken out and left for 3 hours prior to usage. Pt, Au, Ni, Sn, Ti, Dimensionally Stable Anode (DSA, Ru oxide coated on Ti) and glassy carbon plates were tested as the counter electrodes. Prior to usage, all metal foils are cleaned by sonication in methanol except for In foil and Hg amalgam, which were only rinsed with methanol. The reference electrode was Ag/Ag^+ (0.1M $TBABF_4$ + 0.01M $AgNO_3$) in acetonitrile. The electrolytes were all prepared in the glove box and taken out sealed until transferred to the electrochemical cell. For the electrolyte, sodium perchlorate (and other respective supporting electrolytes) were dissolved in 10ml methanol at the required concentrations, transferred into the reaction cell and then purged with Ar gas or CO_2 gas for 10 minutes prior to reaction. During purging, the gas is passed through a moisture trap consisting of molecular sieves and silica beads. The headspace of the cell was determined to be 65cm3, and was ventilated with CO_2 gas and then sealed tightly under CO_2 at atmospheric pressure. All reactions were performed at room temperature under vigorous stirring of the electrolyte. After electrolysis, 0.1ml of the headspace gas was transferred by syringe for gas chromatography (GC) analysis. 5ml of the electrolyte is then collected in 10ml headspace vials for gas chromatography-mass spectrometry (GC-MS) analysis.

2.2.3 Analytical Methods

A potentiostat (VSP-300, BioLogic Science Instruments) was used for all voltammetric measurements and bulk electrolysis. All potentials were controlled against the reference electrode. The quantitative measurement of the gas phase from the headspace pf the electrochemical cell was performed by GC (PerkinElmer, Clarus 580 GC). Liquid products in the electrolyte were

detected by GC-MS (Agilent 5977) using the headspace sampler. NMR spectra was also obtained on a Bruker 600MHz NMR spectrometer (Bruker Advance 600) at room temperature.

2.3 Results and Discussions

2.3.1 Defining a Non-Methyl Formate Producing Anode

In order to construct a one-pot system for electrochemical CO_2 reduction experiments in methanol, the anodic reaction of methanol oxidation to methyl formate needs to be suppressed so as to make sure that all methyl formate detected are originating from the cathodic CO_2 reduction reaction. To determine the suitable anode for reaction in a one-pot cell, the anodic material needs to fulfil the following conditions:

1. The anode material does not produce methyl formate as a major reaction.
2. The anodic reaction products should not interfere with the cathodic reaction.
3. In the case of using a sacrificial anode (as Mg is used as a sacrificial anode in electrochemical reactions in organic solvents), the metal ions from the anode should be deposited on the cathode surface.

Prior to tests in the one-pot cell, Pt foil, Au foil, DSA, Ni foil, glassy carbon plate, Sn foil and Ti foils were tested as the counter electrode in a custom made H-cell, with the catholyte and anolyte separated by a Nafion 117 membrane. The catholyte and anolyte were 10ml each 0.5M $NaClO_4$ in methanol. The working electrode used was Sn foil, and the catholyte and anolyte were purged with CO2 prior to experiment so as to simulate the actual environment in later CO_2 reduction experiments. The anolyte was collected after bulk electrolysis at -1.9V vs Ag/Ag^+ after about 10C charged is passed and analysed by GC-MS to determine the methyl formate concentration. The concentrations of methyl formate produced on each respective anode materials were listed and shown in Table 2.1. Methanol partial oxidation is known to occur on Pt and Au, and thus showing the highest methyl formate

concentrations. Methanol partial oxidation to methyl formate also apparently occurred on the DSA, glassy carbon, and Ti foil anodes, especially DSA which showed the highest methyl formate concentration after bulk electrolysis which indicates that methyl formate formation on Ru oxide by methanol oxidation might be even more active than Pt or Au. For these methyl formate producing anodes, dimethoxymethane (DMM) is also detected at high concentrations, which matches with the hypothesis that in methanol oxidation, the fully oxidized state is CO_2. Partial oxidation of methanol occurs on metals that do not adsorb methanol molecules strong enough, which then desorbs from the metal surface as DMM or methyl formate. [67, 68, 69] Since methyl formate concentration is the lowest on Sn and Ti foil anodes, Sn and Ti were further tested in the one pot cell as the counter electrode.

Bulk electrolysis is conducted at -1.9V vs Ag/Ag^+ in CO_2 purged 0.5M $NaClO_4$ methanol electrolyte with Sn cathode and Sn or Ti anode respectively in the one pot cell. When Sn anode is used as the anode, the current increases sharply during bulk electrolysis as seen in Figure 2.1(a). The sharp current increase in current is due to the dissolution of ions from the Sn anode, which consequently is deposited onto the Sn cathode surface, leading to the formation of small particles on the Sn cathode surface, increasing the reaction surface area, and thus the current increases sharply. After the chronopotentiometric measurement is stopped, the Sn anode surface becomes rough and uneven, indication of Sn oxidation, while the Sn cathode surface becomes a darker shade, showing that electrodeposition of Sn ions originating from the Sn anode oxidation has occurred.

For the Ti anode case, there were no sharp current increases during the bulk electrolysis. In contrast to the Sn anode case, this indicates that no ion deposition on the Sn cathode surface has occurred. Bulk electrolysis in Ar and CO2 purged electrolytes were conducted respectively at the same potential. After 10C charge is passed, the electrolyte is then analysed by GC-

MS. The concentration of methyl formate observed for Ar purged electrolyte was 0.006mM, which is much lower than that observed for CO_2 purged condition (0.1mM). This clearly indicates that methanol oxidation to methyl formate barely occurred on Ti surface (shown by the Ar purged case) and majority of the methyl formate observed originated from CO_2 reduction (shown by the CO_2 purged case). The major reaction that occurred was deduced to be complete methanol oxidation to CO_2 gas, as shown by the appearance of CO_2 peak after bulk electrolysis in Ar purged 0.5M $NaClO_4$ methanol in the GC spectrum shown in Figure 2.3. Furthermore, the originally shiny, metallic grey Ti anode surface after bulk electrolysis became coated with a layer of multi-coloured oxide, as is often observed when Ti electrochemical anodization is done depending on the applied potential. There were also black dots and lines on the Ti anode surface and the edges of the anode appeared to be corroded, with small black particles that could be observed falling off the Ti anode during bulk electrolysis. It is deduced that in the presence of perchlorate ions and in methanol solvent, the Ti oxide layer that is formed during the electrochemical reaction is pitted and corroded easily, and thus the oxide falls off as black TiO_x particles when an oxidizing current is applied. [70]

Based on these experimental results, Ti foil was selected as the anode material for all electrochemical CO_2 reduction experiments in methanol electrolyte.

(a)

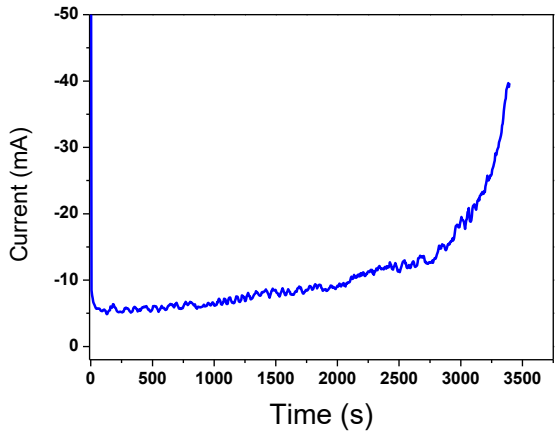

(b)

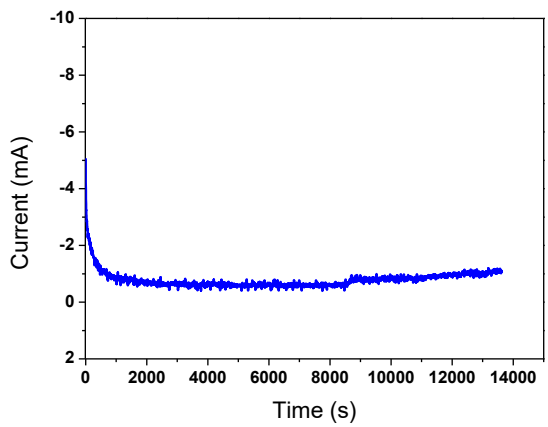

Figure 2.1 Chronopotentiometric measurements at -1.9V vs Ag/Ag^{+} with Sn cathode and (a) Sn anode, in which a sharp current increase is observed, indicating Sn ion deposition on the Sn cathode surface and (b) Ti anode, where no sharp increases in current is observed, indicating that no ion deposition occurred on the Sn cathode surface.

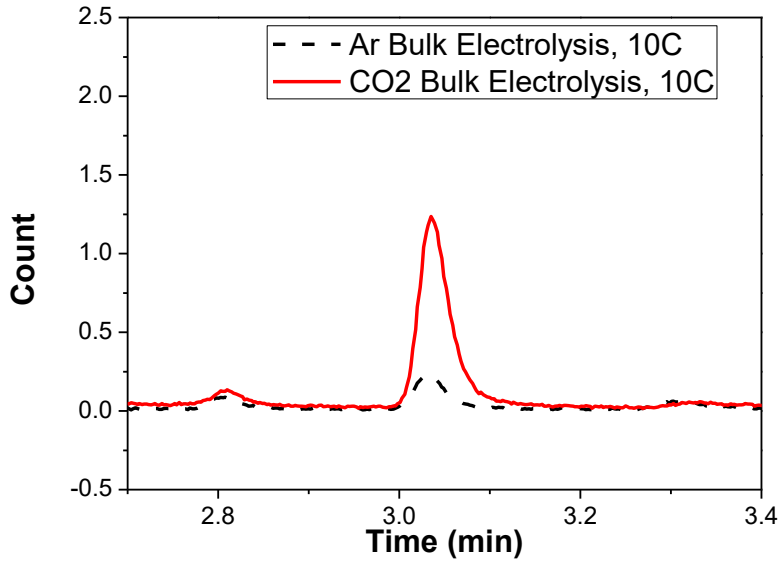

Figure 2.2 GC spectrum showing methyl formate peaks at retention time of 3.05min for Ar and CO_2 purged electrolytes respectively after bulk electrolysis at -1.9V vs Ag/Ag^+ and 10C charge has passed. The concentration of methyl formate for the Ar purged condition was 0.009mM, while for the CO_2 purged condition was 0.6mM.

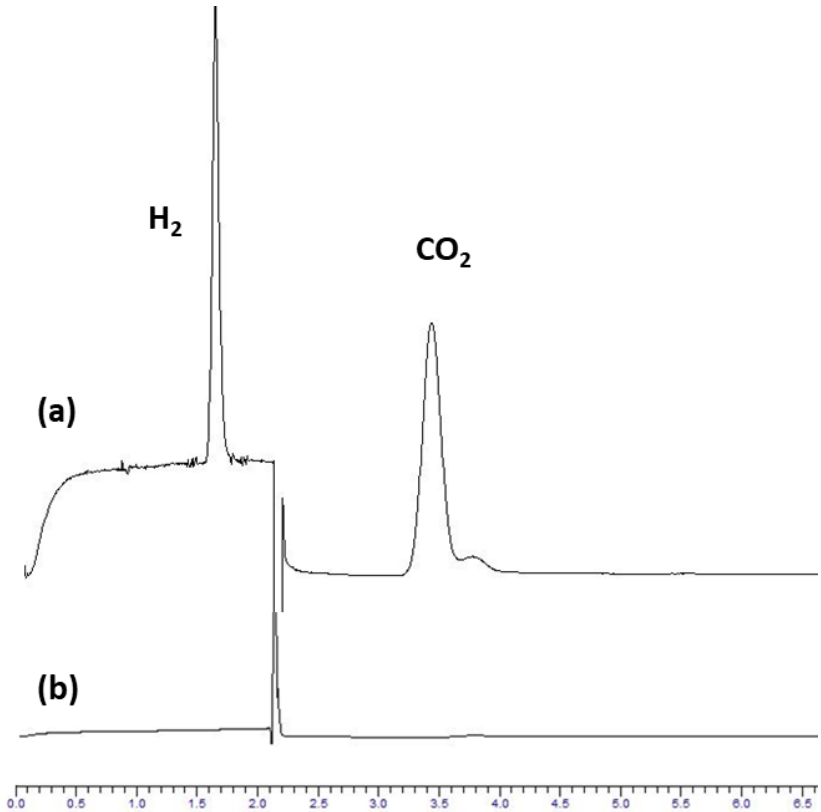

Figure 2.3 GC spectrum showing gas products (a) before and (b) after bulk electrolysis in Ar purged 0.5M NaClO4 methanol with Sn cathode and Ti anode at -1.9V vs Ag/Ag^{+} after 10C charge is passed.

Anode Material	Charge Passed (C)	Methyl Formate Concentration (mM)
Pt foil	12	1.962
Au foil	10	1.852
Ni foil	10	0.981
DSA	10	2.119
Graphite	10	1.108
Sn foil	10	0.064
Ti foil	15	0.105

Table 2.1: Methyl formate concentration produced on various anodic materials in the anolyte after the respective amount of charge is passed. Among the tested materials, Sn and Ti foil showed methyl formate concentration of one order lower than other anodic materials.

2.3.2 Defining a Methyl Formate Producing Cathode Material

According to previous papers, methyl formate formation at high pressure condition was reported in a number of other transition metal catalysts, especially Cu. To demonstrate the effects of the type of transition metal catalyst and to show that methyl formate formation forms through the formate / formic acid pathway, chronoamperometric measurements at -1.0mA for 10C in 0.5M $NaClO_4$ methanol on various transition metal catalysts (Ti, Au, Pb, In, Hg, Sn, and Cu). The tested transition metal catalysts could be divided into 4 categories. Ti represents the transition metal which is not active in CO_2 reduction, Au represents the CO producing metals, Cu represents the hydrocarbon producing metal and Pb, In, Hg and Sn are formate producing metals. The products distribution of the chronoamperometric measurement is shown in Figure 2.4. Methyl formate current efficiency was the highest on Sn surface (7.7%), followed by Cu (6.6%). The current efficiencies of methyl formate for the remaining transition metals were observed at 2% and below. For the non-CO_2 reduction active Ti electrode, no methyl formate formation was observed, and almost 100% of the current efficiency observed was HER. In the case of CO producing Au, barely 1% of methyl formate was observed. The formation of methyl formate was hypothesized to form through the reaction between an adsorbed formate intermediate with methanol, thus various formate producing metals were tested as the cathode, inclusing Pb, In, Hg and Sn. For all formate producing metals, methyl formate was observed at some level, with Sn showing the highest Faradaic efficiency among the other transitions metals. Interesting, Cu also showed Faradaic efficiency for methyl formate at only that slightly lower than Sn, even though Cu is known for hydrocarbon formation. As Sn exhibited the highest Faradaic efficiency, Sn was selected as the cathode material for all further experiments.

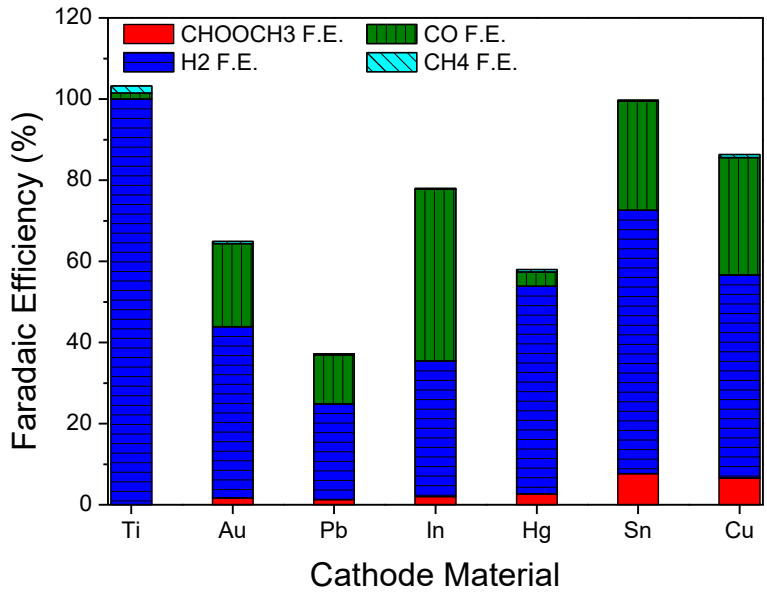

Figure 2.4: Product distribution of chronoamperometric experiments at -1.0mA in CO_2 purged 0.5M NaClO4 methanol after 10C charge is passed on Ti, Au, Pb, In, Hg, Sn and Cu.

2.3.3 Formation of Methyl Formate from CO2 Reduction on the Cathode

To confirm that the methyl formate formation occurred on the Sn cathode surface by CO_2 reduction, bulk electrolysis on Sn cathode with Ti anode in one pot cell in $^{13}CO_2$ purged 0.5M $NaClO_4$ methanol was conducted. The liquid products were analysed by GC-MS and the methyl formate mass spectrums of normal $^{12}CO_2$ purged and isotopic $^{13}CO_2$ purged electrolytes were compared, as shown in Figure 2.5. The methyl formate molecule is comprised of a formate part originating from formic acid and a methoxy part originating from methanol. In the mass spectrum of methyl formate, the 29 mass to charge ratio (m/z) peak corresponds to the formate part (CHO^+), the 31 m/z ratio peak corresponds to the methoxy part (OCH_3^+) and the 60 m/z ratio peak corresponds to the whole molecule ($CHOOCH_3^+$). When an isotopic ^{13}C atom from $^{13}CO_2$ is present in the molecule, the 30 m/z peak is observed at a larger ratio compared to when only $^{12}CO_2$ is present, since the CHO^+ is expected to originate from CO_2 reduction to HCOOH or $HCOO^-$. Also, the 61 m/z peak ratio is also expected to be increased when an isotopic ^{13}C atom is present. Thus as seen in Figure 2.5, the 61/60 m/z peak ratio in the $^{13}CO_2$ purged electrolyte (7.2) is largely increased in comparison with $^{12}CO_2$ purged electrolyte (0.02). Similarly, for the 30/29 m/z peak ratio, in the $^{13}CO_2$ purged electrolyte the ratio was increased to 1.28 in comparison with the 0.13 ratio observed for the $^{12}CO_2$ purged case. Meanwhile, the 32/31 m/z peak ratio in both cases remains unchanged. This provides direct evidence that CO_2 is incorporated into the structure of methyl formate by reduction on Sn cathode to formate, which then reacts with methanol to form methyl formate, and that little to none of the methyl formate observed is originating from the anodic reaction.

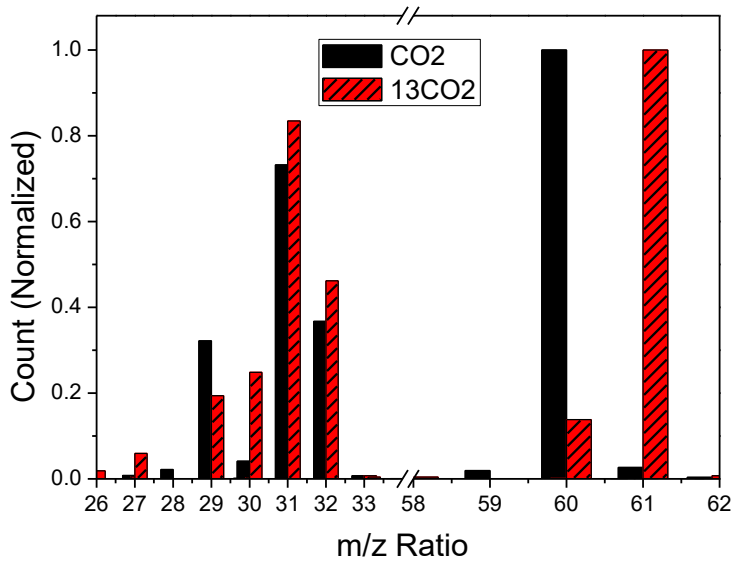

Figure 2.5: Comparison of methyl formate mass spectrum of $^{12}CO_2$ and $^{13}CO_2$ purged electrolyte. The mass/charge ratio peak at 29 corresponds to the formate part (CHO^+) of the methyl formate molecule, while the 60 m/z peak corresponds to the whole methyl formate molecule. The presence of isotopic 13C results in the 30 and 61 m/z peak.

2.3.4 Electrochemical CO_2 Reduction on Sn

The activity of Sn in electrochemical CO_2 reduction in 0.5M $NaClO_4$ is confirmed by cyclic voltammetry (CV). The CV curves for Ar purged and CO_2 purged electrolytes respectively are compared. As shown in Figure 2.6, the activity of Sn in electrochemical CO_2 reduction in methanol is confirmed by the significant current differences between the Ar purged and CO_2 purged conditions. The reduction peak at -1.3V and the oxidation peak at -1.1V observed in the Ar purged condition is predicted to be related to Sn oxidation and reduction. When the electrolyte is purged with CO_2, the redox peaks could not be observed. The current levels between Ar and CO_2 purged conditions differs mainly in the range of -1.9V to -2.5V, which then becomes similar with each other from -2.5V to -3.0V.

Bulk electrolysis at the potential range of -1.9V to -3.0V vs Ag/Ag^+ in CO_2 purged electrolyte was conducted. The product Faradaic efficiencies distribution is shown in Figure 2.7. In the range of -1.9V to -2.5V vs Ag/Ag^+, the Faradaic efficiency of H_2 and CO decreases with more negative applied potentials, but the Faradaic efficiency of methyl formate remained fairly unchanged according to the applied potential at 11% to 13%, with the highest value observed at 13.8% at -2.0V. The Faradaic efficiency of methyl formate appeared to be fairly unaffected by applied potential in this potential range. The formation of methyl formate in this potential range appears to be reflected by the crossover shape in the CV curve in the same potential range. The crossover shape of the CV curve was suggested to be due to the strong adsorption of a CO_2 intermediate species and methanol to form methyl formate. In the potential range of -2.3V to -2.7V, a large dip in total product Faradaic efficiencies could be observed. This could be due to the formation of other products not detected by GC and GC-MS analysis. For potentials more negative than -2.5V, hydrogen evolution steadily increased, and reached 100% at -3.0V. This behaviour was also reflected by the CV current levels

that got increasingly similar between Ar and CO_2 purged conditions in the same potential range of -2.5V to -3.0V. Methyl formate Fardaic efficiency also decreased when potentials more negative than -2.5V was applied. Thus it was suggested that -1.9V to -2.5V is the CO_2 reduction active potential range, while potentials more negative than -2.5V is only hydrogen evolution region.

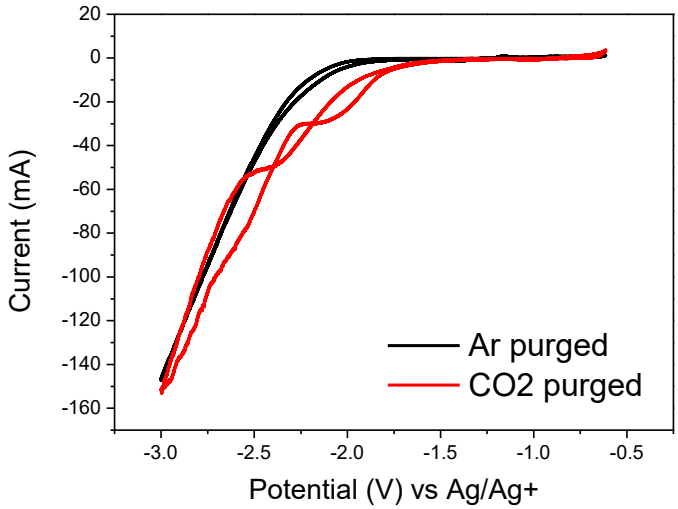

Figure 2.6: Cyclic voltammetry (CV) curves comparison in Ar and CO_2 purged 0.5M $NaClO_4$ methanol on Sn cathode and Ti anode. The scan rate was 0.05V/s and the cycle shown was the 8^{th} cycle.

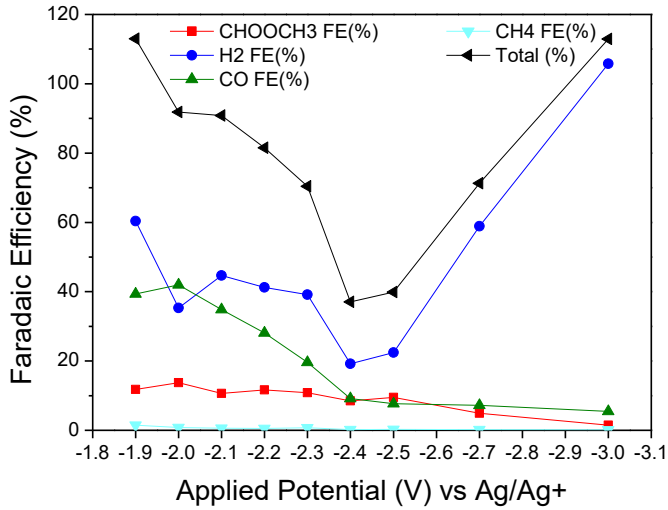

Figure 2.7: Product Faradaic efficiencies distribution of CO_2 reduction on Sn cathode in 0.5M $NaClO_4$ methanol. The products are represented by ■ $CHOOCH_3$; ●H_2; ♦CO; ▲CH_4; ★ total Faradaic efficiency.

2.3.5 Effect of Water Concentration

The presence of water in the electrolyte is observed to have an effect on methyl formate formation. The effect of water concentration was investigated by the systematic addition of water into the methanol electrolyte until 1M prior to bulk electrolysis. The product distribution is shown in Figure 2.8. In Figure 2.8(a) the product distribution of $CHOOCH_3$, H_2 and CO are shown according to increasing water concentration. The Faradaic efficiency of $CHOOCH_3$ decreased significantly from 13% when no water is added to 2% when 1M of water is added as shown in Figure 2.8(b). Also, the Faradaic efficiency for H_2 gas increased from 35% when no water is added to 73% when 1M water is added as shown in Figure 2.8(c), while the Faradaic efficiency of CO decreased from 41% when no water is added to 17% when 1M water is added as shown in Figure 2.8(d). This directly shows that the presence of moisture is detrimental to the formation of methyl formate due to the competing reactions between hydrogen evolution reaction (HER) and CO_2 reduction. Since the deprotonation of water is easier than methanol, deprotonation of water in addition to the deprotonation of methanol to form H_2 competes and becomes more active when more water is present in the electrolyte, thus decreasing the current efficiencies of the CO_2 reduction products. This shows the drying of the reactants need to be done thoroughly prior to the experiments. Therefore, the purchased methanol was not used as received, but was treated with 3°A molecular sieve at 20% volume ratio for more than 48 hours to keep the water content below 19ppm. [71] Also, the sodium perchlorate used was also dried at 220℃ in ambient atmosphere (well below 400℃, in which the decomposition of ClO_4^- to Cl^- occurs) for more than 24 hours prior to usage. [72]

(a)

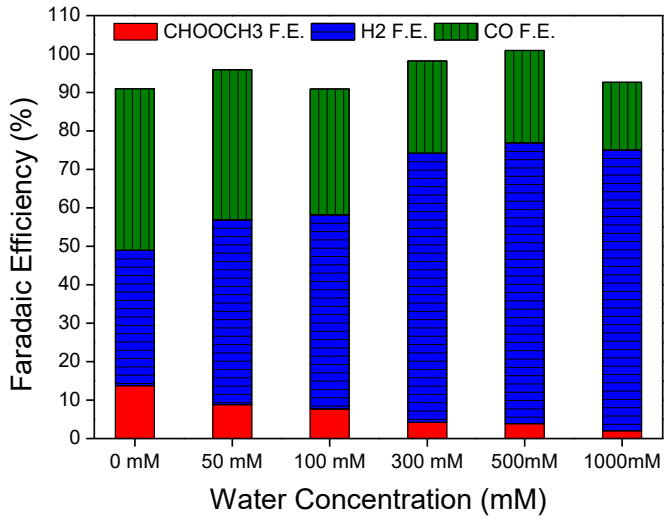
CHOOCH3 F.E.
H2 F.E.
CO F.E.
Faradaic Efficiency (%)
0
10
20
30
40
50
60
70
80
90
100
110
0 mM
50 mM
100 mM
300 mM
500mM
1000mM
Water Concentration (mM)

(b)

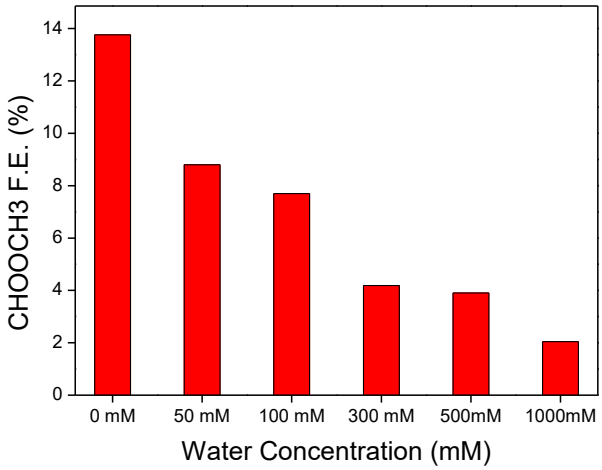
CHOOCH3 F.E. (%)
0
2
4
6
8
10
12
14
0 mM
50 mM
100 mM
300 mM
500mM
1000mM
Water Concentration (mM)

(c)

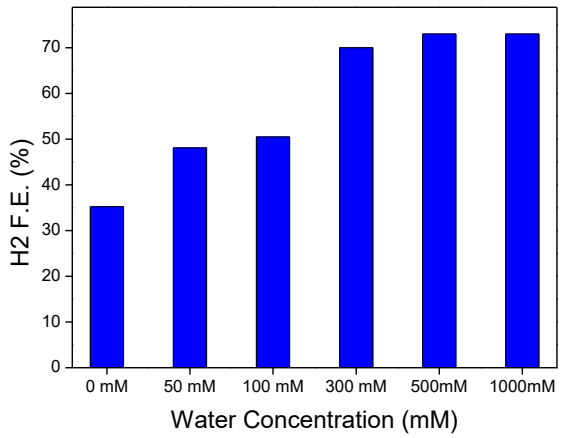

(d)

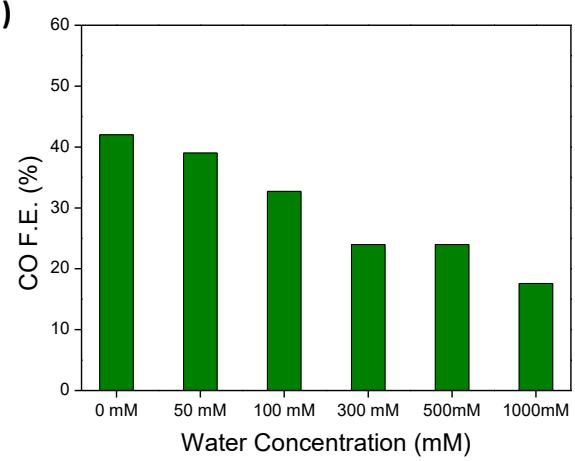

Figure 2.8: Product Faradaic efficiencies distribution of CO_2 reduction on Sn according to the concentration of water added prior to bulk electrolysis from 0M to 1M in 0.5M $NaClO_4$ methanol. (a) shows the all the product distributions of H_2, CO and $CHOOCH_3$, (b) shows the Faradaic efficiency of $CHOOCH_3$, (c) shows the Faradaic efficiency of H_2 and (d) shows the Faradaic efficiency of CO according to increasing water concentration. Bulk electrolysis was conducted at -2.0V vs Ag/Ag^+ until 10C charge has passed.

2.3.6 Effect of Supporting Electrolyte

The type of supporting electrolyte used in an electrochemical reaction can affect the reaction and product distribution, depending on the type of the cation and the anion. While it is well known the size of the cation strongly affects the reaction on the cathode surface during electrochemical CO_2 reduction, the anion is often regarded as not having a significant effect on the cathodic reaction due to repulsion between negative charges of the cathodic surface and the anion itself. There were however instances that showed that the type of anion used can also affect the cathodic surface reaction. Thus, the effects of the cation species and also the anion species are both investigated in this research.

2.3.6.1 Cation Effect

The effect of the type of cation used was investigated by changing the type of cation of a perchlorate salt. For metallic cation perchlorate salts, $LiClO_4$ and $NaClO_4$ were tested. Larger cation sizes such as $KClO_4$ could not be dissolved in methanol solvent. Organic cation $TBAClO_4$ salt was tested. Other smaller organic cation salts such as $TEAClO_4$ were not available. CV experiments were conducted at 0.01V/s for 0.1M LiClO4, NaClO4, and $TBAClO_4$ in methanol. The cation radii of the tested cations increase in the order of $Li^+ < Na^+ < TBA^+$. As shown in Figure 2.10, the current levels for Na^+ is the highest in comparison with Li^+ and TBA^+. Furthermore, for the Na^+ CV curve an observable decrease in current in the reverse (positive) scan, in comparison with the forward (negative) scan can be seen. Barely any bubbles could be observed emanating from the cathode surface during scan at more negative potentials for Na^+ and Li^+, but significant bubbling could be observed for TBA^+. Further experiments by bulk electrolysis in each of the CO_2 purged electrolytes were conducted and the reaction products were analysed when 10C charge is passed. The product distribution is shown in Figure 2.10. The Faradaic efficiency for methyl formate was also the highest

for $NaClO_4$ (7.8%), compared to $LiClO_4$ (3.8%) and $TBAClO_4$ (0%). In the case of TBAClO4, barely any CO_2 reduction products were observed. HER occurred at closely to 100% current efficiency, which is in contrast to previous papers utilizing $TBAClO_4$ at high pressure conditions that reported active CO formation due to the promoting effect of TBA^+ cations. The cathode surface when reaction is conducted at ambient pressure conditions however appeared to be completely different from that at high pressure conditions. The CO_2 surface coverage on the cathode surface at ambient pressure conditions is only approximately one fifth by CO2 concentration in comparison to that at 40atm. [58] Furthermore, simulation data by Ringe et. al. for cation effects on CO production on Ag and also C_2 production on Cu in aqueous electrolyte suggested that for metallic cations, bigger cation sizes results in smaller hydrated cation radius, thus the smaller effective interfacial cation radius. The smaller effective interfacial cation radius leads to increased cation concentration on the cathode surface, which increases the surface charge density and the interfacial electric field, thus driving the adsorption of CO_2 molecules. [73] If the same model for aqueous system can be similarly applied in the methanol solvent, it appears that the highest methyl formate current efficiency could be a result of the smallest effective cation radius in comparison with Li^+ and TBA^+ shown by the hydrated cation radius comparison in Figure 2.11 and data in Table 2.2. The smallest effective interfacial cation radius of Na^+ cations could have let to greater adsorption of CO_2 molecules on Sn cathode surface, resulting in greater methyl formate current efficiencies, while the largest effective interfacial cation radius of TBA^+, which is often considered as non-hydrated, may have resulted in the ineffective adsorption of CO_2 on the surface of Sn cathode, resulting in prevalent HER.

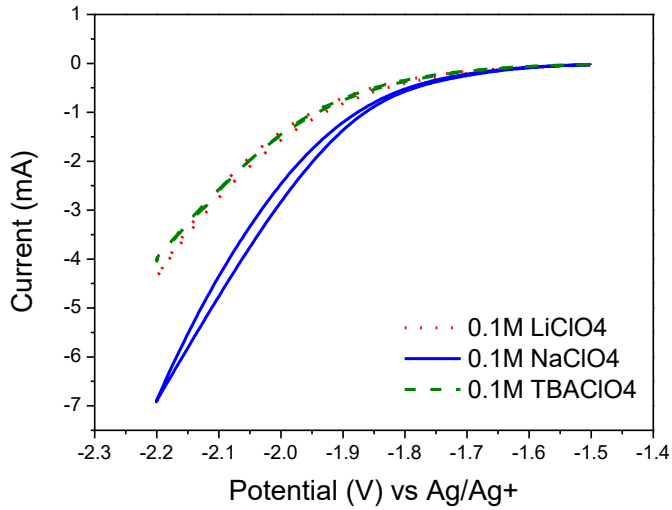

Figure 2.9: CV curves for CO_2 purged 0.1M LiClO4, NaClO4 and TBAClO4 in methanol at scan rate 0.05V/s. The displayed cycle is the 8^{th} cycle.

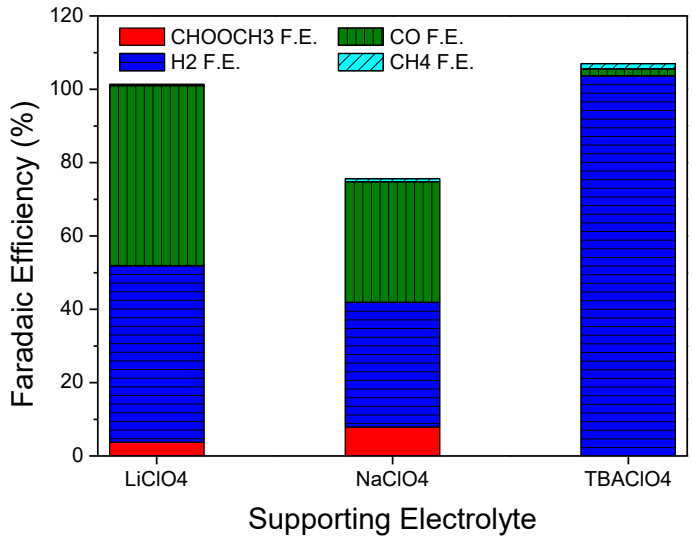

Figure 2.10: Product distribution of bulk electrolysis in CO2 purged 0.1M LiClO4, NaClO4 and TBAClO4 methanol on Sn cathode at -2.0V vs Ag/Ag^{+}. Products are analysed when 10C charge is passed.

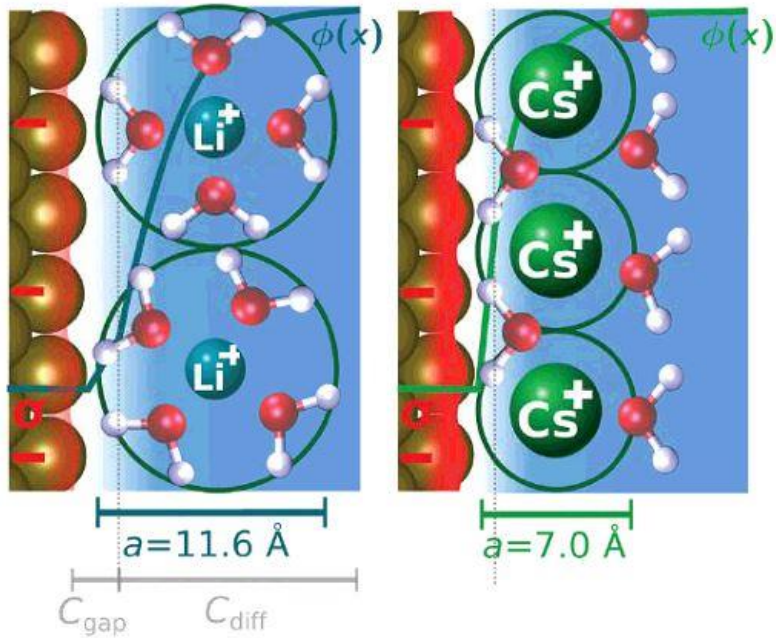

Figure 2.11: Scheme obtained from REF [40] showing the bigger hydrated cation radius of smaller cations such as Li^+, while the bigger cations such as Cs^+ results in smaller hydrated cation radius.

Cation	Effective Interfacial Cation Radii (Å)
Cs	3.5
Rb	3.9
K	4.1
Na	5.2
Li	5.8
TMA	7.8
TEA	8.0
TPA	8.1
TBA	8.4

Table 2.2: Data obtained from REF [40] displaying the effective cation radii (Å), showing the decreasing effective interfacial cation radii with increasing metallic cationic radius, and increasing effective interfacial cation radii with increasing organic cation radius.

2.3.6.2 Anion Effect

To investigate the effect of the type of anion on CO_2 reduction in methanol on Sn surface, various types of Na salts were dissolved and tested. Among the tested Na salts, only ClO_4^-, Cl^-, CH_3O^-, OH^- and BF_4^- salts could dissolve in methanol, while SO_4^{2-}, NO_3^- and HCO_3^- salts could not be dissolved in methanol. Thus bulk electrolysis in CO_2 purged 0.1M $NaClO_4$, NaCl, $NaOCH_3$, $NaBF_4$ and NaOH methanol were conducted. In the case of NaOH, bulk electrolysis could not proceed due to the growth of a thick current passivating Ti oxide layer on the Ti anode surface, thus not data was collected for NaOH. The bulk electrolysis product distribution at -2.0V, 10C is shown in Figure 2.12. The methyl formate current efficiency for NaBF4 was observed to be the highest (29%), followed by $NaClO_4$ (7.8%), $NaOCH_3$ (1.3%) and NaCl (0%). In the case of NaCl, the electrolyte turns brownish yellow during bulk electrolysis due to chlorine evolution on the Ti anode. The dissolved chlorine appears to inhibit CO_2 reduction on the cathode surface, as can be seen by the large increase in HER and barely any CO_2 reduction products were observed. Only 1.3% of methyl formate was observed when $NaOCH_3$ was used as the electrolyte, which could be due to the reaction between methoxide species and formate / formic acid. Higher concentrations of $NaOCH_3$ were also attempted, but concentrations greater than 0.1M resulted in the precipitation of white Na_2CO_3 solid particles during CO_2 purging, thus bulk electrolysis could not be conducted.

$$2\ CH_3ONa + CO_2 + H_2O \rightarrow 2\ CH_3OH + Na_2CO_3$$

The surprisingly dramatic methyl formate Faradaic efficiency observed when $NaBF_4$ was used as the supporting electrolyte was suggested to be due to the weak coordinating ability of BF_4^- anions. The initial results of methyl formate formation observed only when $NaClO_4$ was used as the supporting electrolyte was hypothesized to be due to the simultaneous reduction of perchlorate anions on the cathodic Sn surface, which acts as a

promoter species for the formation of methyl formation. However, it appears that ClO_4^- anions are also included in a series of anionic species named the non-coordinating or weakly coordinating anions. [74] These anionic species, including BF_4^-, PF_6^-, $B(C_6F_5)^-_4$, and $Al[OC(CF_3)_3]^-_4$ interact only weakly with cations. Thus, it was newly suggested that the little to none interaction of the anionic species on the cathodic surface instead, favoured the formation of methyl formate from CO_2 reduction on Sn surface. ClO_4^- though considered as a weakly coordinating anions, could possibly had some interaction on the cathodic surface, which led to the crossover shape of the CV curve in CO_2 purged conditions. To further verify that the largely increased methyl formate Faradaic efficiency was indeed due to the cathodic CO_2 reduction reaction, isotopic $^{13}CO_2$ experiment was again conducted and the mass spectrum was analysed as shown in Figure 2.13. Similar to the mass spectrum observed in $NaClO_4$ electrolyte, the 61/60 m/z peak ratio and 30/29 m/z peak ratio was greatly increased when $^{13}CO_2$ was used instead of $^{12}CO_2$, directly showing that the methyl formate observed originated from the cathodic CO_2 reduction and that the change in supporting electrolyte did not lead to prevalent methyl formate formation on the anode. Furthermore, potential dependency experiments were done in 0.1M $NaBF_4$ and the product distribution is shown in Figure 2.14. The products after 10C charge is passed during bulk electrolysis were analysed at potential range of -2.2V to -2.7V vs Ag/Ag^+. Similar to when $NaClO_4$ was used as the supporting electrolyte, only methyl formate, CO, CH_4 and H_2 were observed as the reaction products. The Faradaic efficiency of methyl formate increased dramatically from -2.2V onwards, and reached a highest efficiency of 79% at -2.5V vs Ag/Ag^+. More negative potentials caused the Faradaic efficiency of methyl formate to decrease. It appeared that methyl formate formation in $NaBF_4$ / methanol electrolyte is stable over a wide range of applied potentials. The Faradaic efficiency of H2 was also markedly lower than that observed in $NaClO_4$ / methanol electrolyte, at an average efficiency of 20% in the same applied

potential range. More research efforts are required to understand this interesting effect of BF_4^- anions, or weakly coordinating anions on increasing the Faradaic efficiency of methyl formate on Sn cathode, and also to uncover the reaction mechanism.

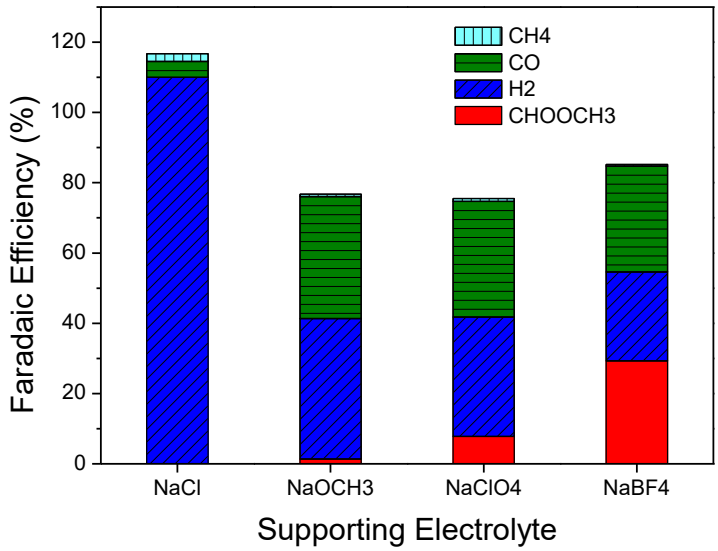

Figure 2.12: Product distribution of bulk electrolysis at -2.0V vs Ag/Ag^{+} in CO_2 reduction in 0.1M $NaClO_4$, NaCl, $NaOCH_3$ and $NaBF_4$ methanol respectively after 10C charge has passed.

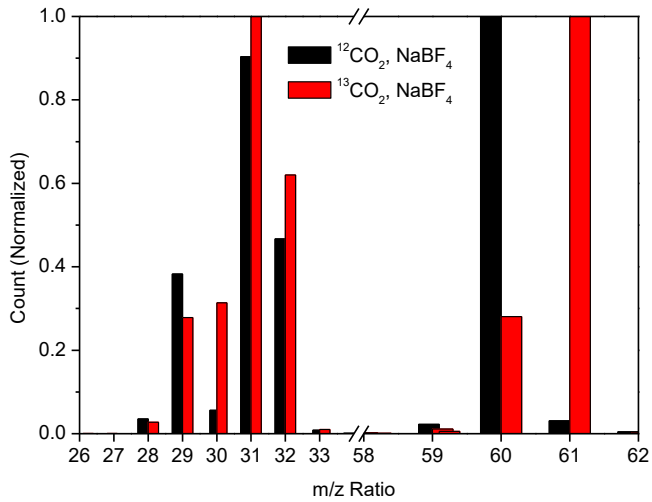

Figure 2.13: Mass spectrum of methyl formate formed from $^{12}CO_2$ (black) and isotopic $^{13}CO_2$ (red) purged 0.1M NaBF4 methanol electrolyte after 10C charge is passed, at -2.2V vs Ag/Ag^+.

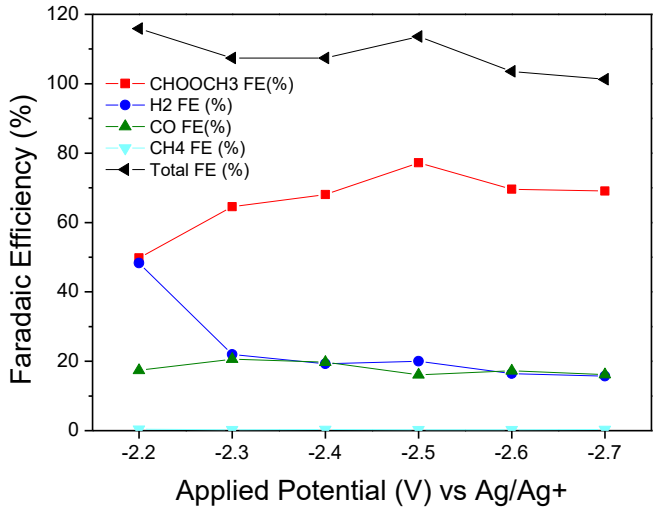

Figure 2.14: Potential dependency and product dependency of CO_2 reduction in 0.1M $NaBF_4$ methanol after 10C charge is passed. The products are represented by ■ $CHOOCH_3$; ●H_2; ♦CO; ▲CH_4; ★ total Faradaic efficiency.

Chapter 3. Conclusion

The combination of the concepts of electrochemical CO_2 reduction and reductive functionalization of CO_2 presents a new perspective of obtaining new reaction products from CO_2 reduction in hopes of improving the economic viability of CO_2 reduction as a chemical process that can be great in practicality and feasibility in pursuit of tackling the problem of global warming. While electrochemical methods are advantageous in terms of reaction tunability, utilization of renewable energy sources, reaction at mild conditions and the utilization of heterogeneous catalysts that can be designed and engineered for well performance in terms of high stability, high selectivity and recyclability, electrochemical CO_2 reduction in aqueous electrolyte has been met with a bottleneck in terms of producing value-added products such as ethylene at high Faradaic efficiencies at low overpotentials, and while the production of formic acid and carbon monoxide is economically viable, these products require special handling and extra processing steps. Thus, we suggest the electrochemical reduction of CO_2 in methanol at ambient pressure and temperature to produce methyl formate as a form of CO_2 reductive functionalization and for easy product separation from the solvent, in addition to the formation of the value added product methyl formate.

First of all, previous reports on electrochemical CO_2 reduction in methanol that reported methyl formate formation were conducted in a one pot cell, and thus a significant portion of the methyl formate observed could possibly originate from the anodic methanol oxidation to methyl formate on Pt. Thus we started off by defining a new one-pot reaction system utilizing Ti as the anode (counter electrode), on which methanol complete oxidation to

CO_2 and Ti surface oxidation to solid oxide particles that falls off the anode surface occurs. Thus the methyl formate observed in our experiments originated from CO_2 reduction at the cathode surface, which is further confirmed by isotopic $^{13}CO_2$ experiments.

Utilizing the newly defined Ti anode, one-pot cell system, comparisons with other transition metal catalysts were done to determine the cathode material for CO2 reduction to methyl formate. It was proposed that methyl formate formation from CO_2 reduction occurs through a formate intermediate pathway, in which the formate intermediate reacts with methanol to form methyl formate. As predicted, on non CO_2 reduction active (Ti) and CO producing (Au) metals, methyl formate was barely or not formed at all. Among the formate producing metals, only Sn showed the highest methyl formate current efficiency, while Pb, In and Hg showed only low levels of methyl current efficiency. Cu also showed methyl formate current efficiency only slightly lower than that of Sn. Since Sn yielded the highest methyl formate Faradaic efficiency, further investigations on electrochemical CO2 reduction in methanol to methyl formate on Sn surface was conducted. It was determined that methyl formate was formed consistently at Faradaic efficiencies of 11% to 13% in the potential range -1.9V to -2.5V vs Ag/Ag^+ in 0.5M $NaClO_4$. The other reaction products observed were gaseous products, which are hydrogen gas, carbon monoxide and methane. The presence of moisture in the electrolyte was determined to be detrimental to the formation of methyl formate as demonstrated by the systematic addition of water prior to bulk electrolysis. To increase the methyl formate Faradaic efficiencies, the effects of cationic species and anionic species of the supporting electrolyte were also investigated. It was discovered that Na^+ showed the highest current efficiency for methyl formate formation in comparison with Li^+ and TBA^+. For the case of the anionic species, it was discovered that BF_4^- anions led to the highest Faradaic efficiency for methyl formate compared to ClO_4^-, Cl^- and

OCH_3^-. Isotopic $^{13}CO_2$ experiment was also done to verify that the methyl formate was formed from CO_2 reduction, and that the change of anionic species to BF_4^- did not lead to changes on the anodic reaction. Potential dependency experiments revealed that methyl formate Faradaic efficiency was observed at the highest of 79% at -2.5V vs Ag/Ag^+ in 0.1M $NaBF_4$ / methanol electrolyte. This sudden dramatic increase in methyl formate Faradaic efficiency was hypothesized to be due to weak to none interaction of weakly coordinating anions such as BF_4^- anions on the cathodic surface. Further experiments are required to understand the effect of weakly coordinating anions on the formation of methyl formate from CO_2 reduction in methanol on Sn surface.

In summary, we proposed a reaction setup to investigate the electrochemical reduction of CO_2 in methanol to produce methyl formate at ambient pressure and temperature conditions. Methyl formate was observed to be formed at high Faradaic efficiencies when $NaBF_4$ is used as the supporting electrolyte and further experiments are required to understand the effect of weakly coordinating anions on the reaction. As an outlook for this research, once a significantly selective catalyst for methyl formate production at high Faradaic efficiencies has been discovered, a paired electrolysis system consisting of concurrent methyl formate production on the cathode by CO_2 reduction and on the anode by partial methanol oxidation can be constructed to produce methyl formate as a value added product, fully utilizing the reaction at both electrodes. Hence we expect further developments and improvements of the current system as a new approach to electrochemical CO_2 reduction.

Reference

1. J. Rogelj. et. al. Paris Agreement climate proposals need a boost to keep warming well below 2℃. *Nature* **534**, 631-639 (2016).
2. Kendra P. Kuhl. et. al. Electrocatalytic conversion of carbon dioxide to methane and methanol on transition metal surfaces. *Journal of the American Chemical Society* **136**, 14107-14113 (2014).
3. H.R. Jhong. et. al. Electrochemical conversion of CO_2 to useful chemicals: current status, remaining challenges and future opportunities. *Current Opinion in Chemical Engineering* **2**, 191-199 (2013).
4. S. Chu. The path towards sustainable energy. *Nature Materials* **16,** 16-22 (2017).
5. D.M. Feng. et. al. Recent advances in transition-metal-mediated electrocatalytic CO_2 reduction: From homogeneous to heterogeneous systems. *Catalysts* **7, 373,** 1-18 (2017).
6. J. E. Pander, et. al. Understanding the heterogeneous electrocatalytic reduction of carbon dioxide on oxide-derived catalysts. *ChemElectroChem* **5,** 219-237 (2018).
7. R. J. Lim. et. al. A review on the electrochemical reduction of CO_2 in fuel cells, metal electrodes and molecular catalysts. *Catalysis Today* **233,** 169-180 (2014).
8. Y. Li. et. al. Heterogeneous catalytic conversion of CO_2: a comprehensive theoretical review. *Nanoscale* **7,** 8663-8683 (2015).
9. J. C. Abanades. et. al. On the climate change mitigation potential of CO_2 conversion to fuels. *Energy and Environmental Science* **10,** 2491-2499 (2017).
10. Y. Hori. Electrochemical CO_2 reduction on metal electrodes. *Modern Aspects of Electrochemistry* **42,** 89-189 (2008).

11. K.D. Yang. et. al. Rise of nano effects in electrode during electrocatalytic CO_2 conversion. *Nanotechnology* **28** (2017).
12. Y. Hori. et. al. Electrocatalytic process of CO selectivity in electrochemical reduction of CO2 at metal electrodes in aqueous media. *Electrochimica Acta* **39,** 1833-1839 (1994).
13. J.P. Jones. et. al. Electrochemical CO_2 reduction: recent advances and current trends. *Israel Journal of Chemistry* **54,** 1451-1466 (2014).
14. Q. Lu. et. al. Electrochemical CO2 reduction: Electrocatalyst, reaction mechanism, and process engineering. *Nano Energy* **29,** 439-456 (2016).
15. B. Kumar. et. al. New trends in the development of heterogeneous catalysts for electrochemical CO_2 reduction. *Catalysis Today* **270,** 19-30 (2016).
16. F. Jia. et. al. Enhanced selectivity for the electrochemical reduction of CO_2 to alcohols in aqueous solution with nanostructured Cu-Au alloy as catalyst. *Journal of Power Sources* **252,** 85-89 (2014).
17. M. Le. et. al. Electrochemical reduction of CO2 to CH_3OH at copper oxide surfaces. *Journal of the Electrochemical Society* **158, 5,** E45-E49 (2011).
18. H. Mistry. et. al. Highly selective plasma-activated copper catalysts for carbon dioxide reduction to ethylene. *Nature Communications* **7,** (2016).
19. R. Kas. et. al. Electrochemical CO_2 reduction on Cu_2O-derived copper nanoparticles: controlling the catalytic selectivity of hydrocarbons. *Physical Chemistry Chemical Physics* **16,** 12194-12201 (2014).
20. P. Hirunsit. et. al. CO2 electrochemical reduction to methane and methanol on copper-based alloys: Theoretical insight. *The Journal of Physical Chemistry C* **119**, 8238-8249 (2015).

21. X. Nie. et. al. Selectivity of CO_2 reduction on copper electrodes: The role of the kinetics of elementary steps. *Angewandte Chemie* **125,** 2519-2522 (2013).
22. Zhou L.Q. et. al. Selective CO_2 reduction on a polycrystalline Ag electrode enhanced by anodization treatment. *Chem Comm* **51,** 17704 (2015).
23. T. Hatsukade. et. al. Insights into the electrocatalytic reduction of CO_2 on metallic silver surfaces. *Physical Chemistry Chemical Physics* **16,** 13814-13819 (2014).
24. Y. Chen. et. al. Aqueous CO_2 reduction at very low overpotential on oxide-derived Au nanoparticles. *Journal of the American Chemical Society* **134,** 19969-19972 (2012).
25. Z. Yin. et. al. Highly selective palladium-copper bimetallic electrocatalysts for the electrochemical reduction of CO_2 to CO. *Nano Energy* **27,** 35-43 (2016).
26. Y. Zhao. et. al. Tin nanoparticles decorated copper oxide nanowires for selective electrochemical reduction of aqueous CO_2 to CO. *Journals of Materials Chemistry A* **4,** 10710-10718 (2016).
27. Choi. S.Y. et. al. Electrochemical reduction of carbon dioxide to formate on tin-lead alloys. *ACS Sustainable Chem. Eng.* **4,** 1311-1318 (2016).
28. W. Lv. et. al. Studies on the faradaic efficiency for the electrochemical reduction of carbon dioxide to formate on tin electrode. *Journal of Power Sources* **253,** 276-281 (2014).
29. S. Mu. et. al. Electrocatalytic reduction of carbon dioxide on nanosized fluorine doped tin oxide in the solution of extremely low supporting electrolyte concentration: Low reduction potentials. *ACS Applied Energy Materials* **1,** 1680-1687 (2018).

30. S. Zhang. et. al. Nanostructured tin catalysts for selective electrochemical reduction of carbon dioxide to formate. *Journal of the American Chemical Society* **136,** 1734-1737 (2014).
31. B. Innocent. et. al. Electro-reduction of carbon dioxide to formate on lead electrode in aqueous medium. *Journal of Applied Electrochemistry* **39,** 227-232 (2009).
32. C. H. Lee. et. al. Controlling H^+ vs CO_2 reduction selectivity on Pb electrodes. *ACS Catalysis* **5**, 465-469 (2015).
33. A. Vasileff. et. al. Bronze alloys with tin surface sites for selective electrochemical reduction of CO2. *Chemical Communications* **54,** 13965-13968 (2018).
34. C. W. Lee. et. al. Selective electrochemical production of formate from carbon dioxide with bismuth-based catalysts in an aqueous electrolyte. *ACS Catalysis* **8,** 931-937 (2018).
35. M. Jitaru. Electrochemical carbon dioxide reduction – fundamental and applied topics (review). *Journal of the University of Chemical Technology and Metallurgy* **42,** 333-344 (2007).
36. S. Ikeda. Selective formation of formic acid, oxalic acid, and carbon monoxide by electrochemical reduction of carbon dioxide. *Bulletin of the Chemical Society of Japan* **60,** 2517-2522 (1987).
37. Y. Tomita. et. al. Electrochemical reduction of carbon dioxide at a platinum electrode in acetonitrile-water mixtures. *Journal of the Electrochemical Society* **147, 11,** 4164-4167 (2000).
38. Y. Oh. et. al. Electrochemical reduction of CO_2 in organic solvents catalysed by MoO_2. *Chemical Communications* **50,** 3878-2881 (2014).
39. Y. Matsubara. et. al. Thermodynamic aspects of electrocatalytic CO_2 reduction in acetonitrile and with an ionic liquid as solvent or electrolyte. *ACS Catalysis* **5,** 6440-6452 (2015).

40. M.C. Figueiredo. et. al. In situ spectroscopic study of CO_2 electroreduction at copper electrodes in acetonitrile. *ACS Catalysis* **6,** 2382-2392 (2016)
41. M. Jouny. et. al. General techno-economic analysis of CO2 electrolysis systems. *Industrial and Engineering Chemical Research* **52,** 2165-2177 (2018).
42. D. Ren. et. al. Tuning the selectivity of carbon dioxide electroreduction toward ethanol on oxide-derived Cu_xZn catalysts. *ACS Catalysis* **6,** 8239-8247 (2016).
43. Y. Huang. et. al. Electrochemical reduction of CO2 using copper single-crystal surfaces: Effects of CO* coverage on the selective formation of ethylene. *ACS Catalysis* **7,** 1749-1756 (2017).
44. L. Mandal. et. al. Investigating the role of copper oxide in electrochemical CO_2 reduction in real time. *ACS Applied Materials and Interfaces* **10,** 8574-8584 (2018).
45. J. B. Greenblatt. et. al. The technical and energetic challenges of separating (Photo)electrochemical carbon dioxide reduction products. *Joule* **2,** 281-420 (2018).
46. S. Sahin. et. al. Investigation of formic acid separation from aqueous solution by reactive extraction: Effects of extractant and diluent. *Journal of Chemical Engineering Data*, **55, 4,** 1519-1522 (2010).
47. M. Rumayor. et. al. Formic acid manufacture: Carbon dioxide utilization alternatives. *Applied Sciences* **8, 914,** 1-12 (2018).
48. A. S. Agarwal. et. al. The electrochemical reduction of carbon dioxide to formate / formic acid: Engineering and economic feasibility. *ChemSusChem* **4,** 1301-1310 (2011).
49. C. D. N. Gomes. et. al. A diagonal approach to chemical recycling of carbon dioxide: Organocatalytic transformation for the reductive functionalization of CO_2. *Angewandte Chemie International Edition* **51,** 187-190 (2012).

50. X.F. Liu. et. al. Transition metal-catalyzed reductive funcationalization of CO_2. *European Journal of Organic Chemistry* 2437-2447 (2019).
51. M. Tamura. et. al. CeO_2-catalyzed direct synthesis of dialkylureas from CO_2 and amines. *Journal of Catalysis* **343**, 75-85 (2016).
52. K. Tomishige. et. al. CO_2 conversion with alcohols and amines into carbonates, ureas, and carbamates over CeO_2 catalyst in the presence and absence of 2-cyanopyridine. *The Chemical Record* **19,** 1354-1379 (2019).
53. C. Federsel. et. al. A well-defined iron catalyst for the reduction of bicarbonates and carbon dioxide to formats, alkyl formats and formamides. *Angewandte Chemie International Edition* **49, 50,** 9777-9780 (2010).
54. J. S. Lee. et. al. Methyl formate as a new building block in C1 chemistry. *Applied Catalysis* **57,** 1-30 (1990).
55. T. Saeki. et. al. Electrochemical reduction of CO_2 with high current density in a CO_2-methanol medium. *Journal of Physical Chemistry* **99, 20,** 8440-8446 (1995).
56. A. Naitoh. et. al. Electrochemical reduction of carbon dioxide in methanol at low temperature. *Electrochimica Acta* **38, 15,** 2177-2179 (1993).
57. T. Mizuno. et. al. Electrochemical reduction of CO_2 in methanol at -30℃. *Journal of Electroanalytical Chemistry* **391,** 199-201 (1995).
58. T. Saeki. et. al. Electrochemical reduction of CO_2 with high current density in a CO_2 + methanol medium, II. CO formation promoted by tetrabutylammonium cation. *Journal of Electroanalytical Chemistry* **390,** 77-82 (1995).
59. T. Saeki. et. al. Electrochemical reduction of CO_2 with high current density in a CO_2 + methanol medium at various metal electrodes. *Journal of Electroanalytical Chemistry* **404,** 299-302 (1996).

60. S. Kaneco. et. al. Electrochemical conversion of carbon dioxide to formic acid on Pb in KOH/methanol electrolyte at ambient temperature and pressure. *Energy* **23, 12,** 1107-1112 (1998).
61. K. Ohta. et. al. Electrochemical reduction of carbon dioxide in methanol at ambient temperature and pressure. *Journal of Applied Electrochemistry* **28,** 717-724 (1998).
62. S. Kaneco. et. al. Electrochemical reduction of carbon dioxide to ethylene with high Faradaic efficiency at a Cu electrode in CsOH/methanol. *Electrochimica Acta* **44,** 4701-4706 (1999).
63. S. Ohya. et. al. Electrochemical reduction of CO_2 in methanol with aid of CuO and Cu_2O. *Catalysis Today* **148,** 329-334 (2009).
64. M. Murugananthan. et. al. Electrochemical reduction of CO_2 using Cu electrode in methanol/$LiClO_4$ electrolyte. *International Journal of Hydrogen Energy* **40,** 6740-6744 (2015).
65. S. Kaneco. et. al. Electrochemical reduction of carbon dioxide on an indium wire in a KOH/methanol-based electrolyte at ambient temperature and pressure. *Environmental Engineering Science* **16, 2,** 131-137 (1999).
66. A. A. Abd-El-Latif. et. al. Formation of methyl formate during methanol oxidation revisited: The mechanism. *Journal of Electroanalytical Chemistry* **662,** 204-212 (2011).
67. J. Munk. et. al. The electrochemical oxidation of methanol on platinum and platinum + ruthenium particulate electrodes studies by in-situ FTIR spectroscopy and electrochemical mass spectrometry. *Journal of Electroanalytical Chemistry* **401,** 215-222 (1996).
68. C. R. Anthony. et. al. Selective electrochemical oxidation of methanol to dimethoxymethane using Ru/Sn catalysts. *Journal of Molecular Catalysis A: Chemical* **227,** 113-117 (2005).

69. S. Wasmus. et. al. Real-time mass spectrometric investigation of the methanol oxidation in a direct methanol fuel cell. *Journal of the Electrochemical Society* **142, 11,** 3825-3833 (1995).
70. E.P. Parry. et. al. Effect of chloride on the anodic dissolution of titanium in methanolic solutions. *Journal of Electrochemical Society: Electrochemical Science and Technology* **119, 9,** 1141-1147 (1971).
71. D. B. G. Williams et. al. Drying of organic solvents: Quantitative evaluation of the efficiency of several desiccants. *Journal of Organic Chemistry* **75,** 8351-8354 (2010).
72. G. G. Marvin. et. al. Thermal decomposition of perchlorates. *Industrial and Engineering Chemistry* **17, 8,** 474-476 (1945).
73. S. Ringe. et. al. Understanding cation effects in electrochemical CO_2 reduction. *Energy and Environmental Science* **12,** 3001-3014 (2019).
74. I. Krossing. et. al. Noncoordinating anions – fact or fiction? A survey of likely candidates. *Angewandte Chemie* **43,** 2066 – 2090 (2004).

국문초록

산업 혁명 이후 대기 중 이산화탄소 농도는 꾸준히 상승하고 지구 온난화 현상을 초래하고 극단적인 기후 변화, 만년설의 융해, 생태계 파괴 및 기타 심각한 환경 문제를 일으키고 있다. 자연계에서 탄소는 생물의 호흡에서 방출되어 광합성을 통해 식물에 의해 재흡수된다. 이산화탄소(CO_2)는 캘빈 사이클(calvin cycle)를 통해 포도당이나 과당 등 당 분자의 구조에 도입된다. 이 생화학 반응으로부터 영감을 얻어, 대기 중 이산화탄소 농도를 절감하고 CO_2를 다양한 유용한 형태로 변환하기 위해 신 재생 에너지를 이용한 인공 전기 화학 CO_2 환원 시스템이 제안되었다고 한다. 전기 화학적 CO_2 환원의 연구는 주로 수계 전해질로 이루어지고 있으며, 주요 반응 생성물은 일산화탄소, 포름산, 메탄올, 메탄 및 에틸렌 또는 에탄올 등의 생성물로 알려져 있다. CO_2 환원을 통해 에틸렌을 생성하기 위해 필요한 전자수는 많으므로 전자 당 가격이 낮아지면서 충분히 높은 패러데이 효율 (Faradaic efficiency)를 아직 달성 못하고 있는 상황에 경제적으로 유리한 반응으로 실행하는 것이 어려운 것이다. 일산화탄소와 포름산은 전자 당 가격이 가장 높은 반면, 일산화탄소는 매우 독성이 높고, 특별한 취급이 필요합니다. 또한 포름산은 물과 아제오트로프 형태 (azeotrope)가 형성되므로 수계 전해질에서 분리하기가 어려운 것이다. 따라서, 새로운 전략으로 C-C, C-N, C-O 결합의 형성을 통해 새로운 CO_2 환원 생성물을 얻기 위해 CO_2 reductive functionalization 를 제안했다. C-O 결합 형성의 경우에는, 고온고압 조건에서 전이 금속 촉매을 이용해 CO_2과 메탄올을 반응시키며 메틸포르메이트를 생성하는 반응이 있다. 화학적 방법 대신에, 전기화학적 방법을 통해 반응 생성물의 조정 가능성, 촉매의 재활용성, 실온 및 대기압 하에 반응 진행이 가능해지므로 화학적 반응보다

우세가 있다. 따라서 메탄올 전해질에서 전기화학적 CO_2 환원으로 가격이 높고 분리하기 간단한 메틸포르매이트를 생성하는 것을 제안한다.

원팟셀(onepot cell)에서 실험을 실행하기 위해 메탄올 산화으로 메틸포르매이트를 생성하지 않는 양극 재료가 선택되었다. 메틸포르매이트로 메탄올의 부분 산화는 백금(Platinum, Pt) 표면에서 일어나는 것으로 알려져 있기 때문에, 전기 화학적 CO_2 환원 시스템에서 일반적으로 사용되는 Pt 양극은 원팟셀에서의 메틸포르매이트를 생성하는 CO_2 환원 반응을 구별해서 관찰하는 것이 어려워지므로 메탄올 전해질에서 Pt 를 양극으로 사용할 수 없다. 티타늄에서는 메틸포르매이트를 작거나 거의 없는 양으로 생성되는 것으로 확인 되며 양극 재료로 선정되었다. 음극 재료를 정하기 위해 CO_2 환원에 반응성이 없거나, 일산화탄소를 생성하거나, 포르매이트를 생성하거나, 탄화수소를 생성하는 구리 (Cu)전이 금속들로 실험 진행을 해 봤더니, 그 중에서 제일 높은 패러데이 효율로 메틸포르매이트를 생성하는 Sn 을 음극 재료로 정했다. CO_2 환원에서 메틸포르매이트 형성을 동위 원소 $^{13}CO_2$ 실험을 통해 직접 확인되었다. 0.5M $NaClO_4$ 메탄올 전해질에서 Sn 음극에서 CO_2 환원 반응 활성을 사이클릭 볼타메트리 (cyclic voltammetry, CV)를 통해 확인되었으며, 메틸포르매이트의 패러데이 효율은 -1.9V 부터 -2.5V vs Ag/Ag^+ 사이에 11%부터 13% 사이로 확인되었다. 수분은 CO_2 환원을 통해 메틸포르매이트 형성에 해로운 것으로 발견되었다. 메틸포르매이트의 패러데이 효율을 높이기 위해 다른 지지 전해질(supporting electrolyte)를 이용해 실험했다. Li^+, Na^+과 TBA^+ 양이온 중에서 Na^+을 이용하면 제일 높은 메틸포르매이트 효율이 나타나기 때문에 Na^+양이온을 고정시키며 음이온을 바꿔서

실험했다. BF_4^- 음이온은 ClO_4^- 음이온에 비해 훨씬 더 높은 메틸포르매이트의 패러데이 효율을 가져온 것으로 발견되었다. 음극 표면에서의 상호 작용이 매우 약하거나 거의 없는 weakly coordinating anions 는 Sn 표면에서 메틸포르매이트 생성에 중요하다는 가설을 새웠으며 0.1M $NaBF_4$ 메탄올 전해질에서 -2.2V 부터 -2.7V vs Ag/Ag^+의 전압을 걸어 실험한 결과 메틸포르매이트의 패러데이 효율은 위 전압 범위에서 69 %에서 79 % 사이로 나온 것으로 확인되었다.

주요어 : 전기 화학적 CO2 환원, 메탄올, 메틸포르매이트, reductive functionalization

학번: 2018-28752